RESEARCH REPORT

on

METALLURGICAL INVESTIGATIONS OF TWO TWO FAILED COMPONENTS

PART ONE: PLUG AND VALVE STEM, PART NO. FW-13A-FCV

PART TWO: STAINLESS STEEL WELD METAL FROM FEEDWATER PIPE

to

NIAGARA MOHAWK POWER CORPORATION

February 17, 1988

by

R. D. Buchheit and T. P. Groeneveld

BATTELLE
Columbus Division
505 King Avenue
Columbus, Ohio 43201-2693

Battelle
Columbus Division
505 King Avenue
Columbus, Ohio 43201-2693
Telephone (614) 424-6424
Telex 24-5454

February 17, 1988

FEDERAL EXPRESS

Mr. T. W. Roman
Station Superintendent
Nine Mile Point Unit #1
P. O. Box 32
Lycoming NY 13093

Dear Mr. Roman:

Attached are two copies of a final report of Battelle's metallurgical investigation of two failures, (1) a fracture of a stem and plug, Part No. FW-13A-FCV, and (2) a cracked weld in pipe from the suction side of the feedwater pump, from the Nine Mile Point Unit #1 Nuclear Station, Lycoming, New York.

Briefly, the results of the investigation of the stem/plug failure indicated that the fracture of the stem at the fillet weld was caused by reverse-bending fatigue induced by wear on the surface of the lower plug. The results of the investigation of the cracked stainless steel weld metal in the feedwater pipe indicated that the failure was caused by intergranular-stress-corrosion-cracking, IGSCC, of sensitized weld-metal grain boundaries. Sensitization of the grain boundaries apparently occurred at the time the pipe was welded since austenitic stainless steel does not become sensitized at the service temperature, which was reported to be 316 F.

Mr. Robert Cushman (NMPC) requested today that the following information in regard to the stem/plug failure be included in this covering letter. The weight of the plug was approximately 61 pounds; the radius of the fillet weld at the threaded joint between the stem and the plug was about 0.4 inch.

Both investigations were very interesting and a pleasure to conduct. If any questions arise concerning the content of the report and/or the results obtained, please do not hesitate to call me at (614) 424-4049.

Very truly yours,

R. D. Buchheit
Principal Research Engineer
Physical Metallurgy Section

xc: Mr. Lee Klosowski (2 copies)
Mr. F. A. Hawksley (covering letter only)

TABLE OF CONTENTS

LIST OF TABLES

LIST OF FIGURES

METALLURGICAL INVESTIGATIONS OF TWO FAILED COMPONENTS

by

R. D. Buchheit and T. P. Groeneveld

from

BATTELLE
Columbus Division

February 17, 1988

INTRODUCTION

Failures of two components occurred at the Nine Mile Point Unit No. 1 Nuclear Station of Niagara Mohawk Power Corporation (NMPC). At the request of NMPC, the Battelle Columbus Division conducted a metallurgical investigation of the failed components to determine, insofar as possible, the most probable cause of each failure.

One of the failures occurred in NMPC Part No. FW-13A-FCV. The part was a component of a feedwater flow-control valve. The other failure occurred in a stainless steel welded pipe joint from the suction side of the feedwater pump. This report consists of two parts which describe the details and results of the metallurgical investigation of each failure, respectively. Part One describes the investigation of the valve stem and plug, Part No. FW-13A-FCV; Part Two describes the investigation of welded feedwater pipe.

PART ONE: PLUG AND VALVE STEM, PART NO. FW-13A-FCV

Introduction

The failed component of NMPC Part No. FW-13A-FCV consisted of a plug and valve stem. The stem was threaded into one end of the plug and fillet-welded circumferentially to the plug at the threaded joint. A sketch of the plug/stem component within the body of the control valve is presented in Figure 1. The location of the failure is indicated in

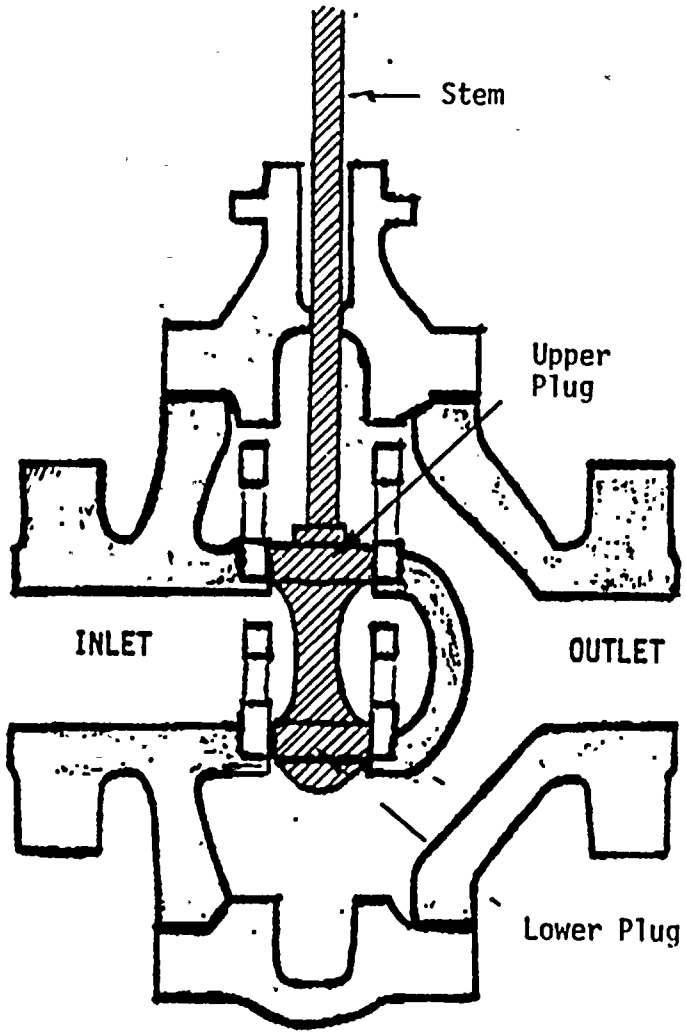

a. Stem/Plug in the Closed Position

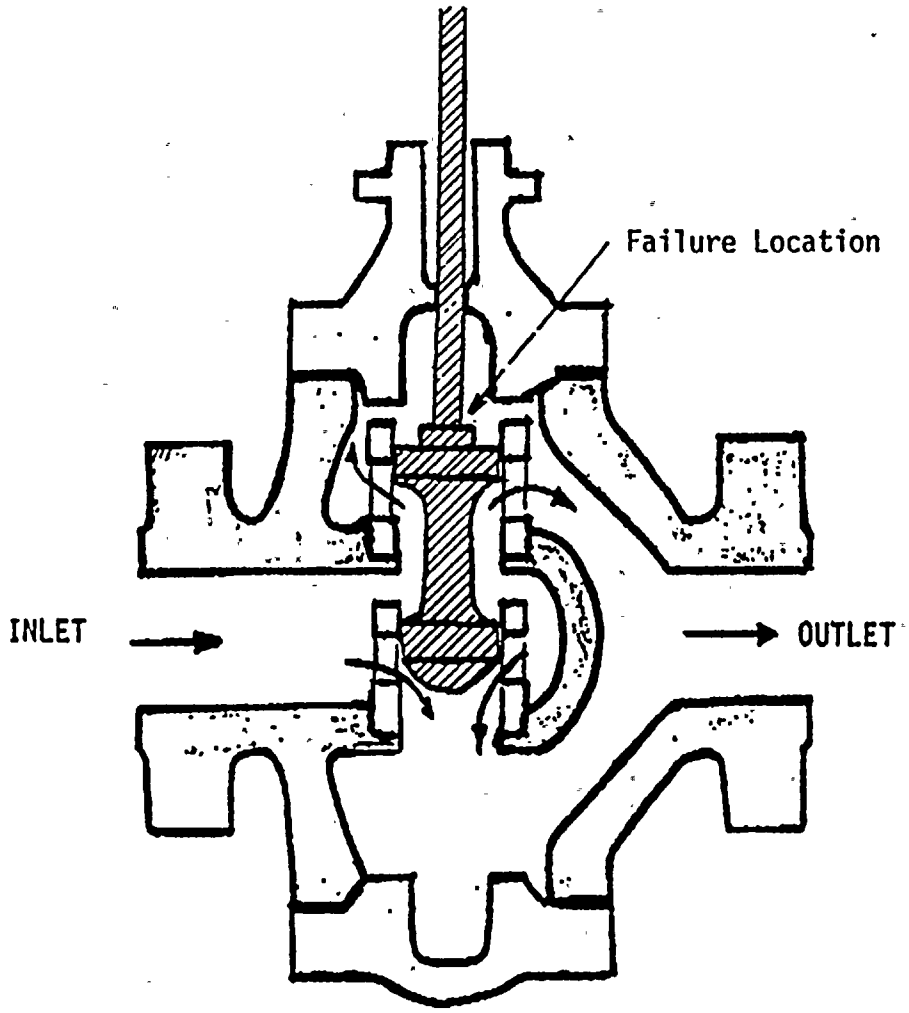

b. Stem/Plug in the Open Position

FIGURE 1. SKETCH OF THE FLOW-CONTROL VALVE SHOWING THE STEM/PLUG COMPONENT, PART NO. FW-13A-FCV (Cross-hatched area) Drawing supplied by NMPC

Figure 1b. The failure was a transverse fracture of the 1-inch-diameter stem through the fillet weld.

The plug was reported to be a stainless steel casting, and the stem and fillet weld-metal also were reported to be stainless steel; however, the type or grades of stainless steel were not reported. The valve controlled the flow of demineralized feedwater back to the reactor at 316 F under a pressure of 1278 psig. The service time of the valve was reported to be from June 1986 to December 1987; the valve operated continuously for 415 days during that period of time.

NMPC submitted the entire fractured stem and plug to Battelle for the metallurgical investigation of the failure.

Summary

A metallurgical investigation of a fracture at the fillet weld between a valve stem and plug (Part No. FW-13A-FCV) was performed to determine the most probable cause of the failure. The investigation involved primarily a chemical analysis of the weld metal, fractographic studies of the crack surface, and metallographic studies of cross sections traversing the cracked region.

The results of the investigation indicated that the crack was a reverse-bending fatigue fracture. A primary and a secondary fatigue crack initiated from opposite sides of the stem, respectively. The regions of the crack origins appeared to be subsurface in weld metal, but no specific initiation sites were identified. The bending stresses were believed to have developed in service as a result of wear on the lower plug. As the depth of the wear increased, the bending stresses probably intensified.

The chemical compositions of the stem and fillet weld indicated those materials to be Type 316 stainless steel. The microstructures of the stem and fillet-weld metal were typical of wrought and annealed Type 316SS, and of Type 316SS weld metal, respectively. The plug was indicated by its chemical composition and microstructure to be an austenitic stainless steel casting designated as cast alloy CF8M.

Recommendations to prevent such failures in the future are: (1) to increase the diameter of the stem and to use a streamline, elliptical, or parabolic form of fillet at the welded joint, and (2) to consider a change of design and/or material for the plug to provide better wear resistance of the lower end of the plug.

Results of Laboratory Examinations

Chemical Analyses

Chemical analyses of the plug, stem, and fillet weld metal were conducted. The chemical compositions of the plug and stem were determined using emission spectrographic analytical techniques; the compotion of the fillet weld-metal was determined using X-ray energy-dispersive (EDS) microprobe analytical techniques in conjunction with the scanning electron microscope. (EDS microprobe analyses can detect elements of atomic number 11, sodium, and higher. The concentrations of the elements detected by that technique are relative and semi-quantitative.) The weld metal was analyzed by EDS because the amount of weld metal required for other analytical techniques was not readily available.

The results of the chemical analyses are presented in Tables 1 and 2. Included in Table 1 are the composition limits for Type 316 stainless steel and cast CF8M stainless steel for comparison with the chemical compositions obtained from the stem and plug, respectively. The composition of the stem satisfied the composition limits of Type 316 stainless steel. Except for the chromium content, the composition of the plug appeared to be more representative of the composition of CF8M, than of the composition of any other cast stainless steel.

As shown in Table 2, the principal elements detected in three areas of the fillet weld metal by EDS were iron, chromium, nickel, and molybdenum. Except for the relative concentration of molybdenum in Area 3, the relative concentrations of those elements were within the composition limits, which are included in Table 2, of AWS E316 stainless steel welding electrode.

TABLE 1. EMISSION SPECTROGRAPHIC ANALYSES OF THE CHEMICAL COMPOSITIONS OF THE STEM AND PLUG

Element	Content, weight percent			
	Stem	316SS[a]	Plug	CF8M[b]
Carbon	0.07	0.08 max	0.06	0.08 max
Manganese	1.71	2.00 max	0.36	1.5 max
Phosphorus	0.034	0.045 max	0.027	0.04 max
Sulfur	0.027	0.03 max	0.023	0.04 max
Silicon	0.59	1.00 max	1.30	2.0 max
Copper	0.25		0.10	
Tin	0.011		0.001	
Nickel	12.1	10-14	9.3	9-12
Chromium	17.8	16-18	16.6	18-21
Molybdenum	2.2	2-3	2.2	2-3
Aluminum	0.000		0.001	
Vanadium	0.05		0.05	
Niobium	0.01		0.006	
Zirconium	0.003		0.004	
Titanium	0.005		0.004	
Boron	0.0004		0.0001	
Calcium	0.0015		0.0012	
Cobalt	0.21		0.071	
Tungsten	0.00		0.00	

(a) Composition limits for wrought Type 316 stainless steel.

(b) Composition limits for cast CF8M stainless steel.

TABLE 2. X-RAY ENERGY-DISPERSIVE MICROPROBE ANALYSIS OF THE FILLET WELD METAL

Element Detected	Relative Concentration, weight percent			AWS[(a)] E316
	Area 1	Area 2	Area 3	
Iron	66.1	66.2	67.2	Bal.
Silicon	0.7	0.6	0.4	0.90 max
Nickel	13.3	13.1	13.1	11.0-14.0
Chromium	17.6	17.7	17.6	17.0-20.0
Molybdenum	2.3	2.4	1.7	2.0-3.0

(a) Composition limits for AWS E316 stainless steel welding electrode.

Therefore, the fillet weld metal was most likely a Type 316 stainless steel.

Fractographic Examinations

Visual and Low-Magnification Stereomicroscopic Examinations.

The stem, plug, and the opposing halves of the fracture surface were examined visually and at low magnifications (7 to 30x) using an optical stereomicroscope.

The macroscopic appearance of each half of the fracture surface is shown in Figure 2. The photomacrographs in Figure 2 are oriented so that the stem-half of the fracture (Figure 2a) matches the plug-half of the fracture (Figure 2b) by folding Figure 2a down on top of Figure 2b.

Although macroscopic fracture features on the left side of the fracture surfaces, as shown in Figure 2, and at many other regions around the periphery of the fracture surface were obliterated by mechanical damage, some fracture features, which were characteristic of fatigue-crack propagation, were evident in the remainder of the fracture surface. Those features were two thumbnail patterns on opposite sides of the stem and a few beach marks. The primary, or larger, thumbnail region is identified by Arrow 1 and the smaller thumbnail region on the opposite

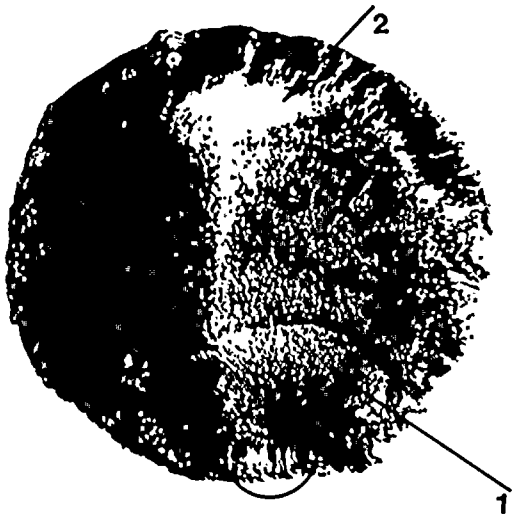

1X 2N723

a. Stem-Half of the Fracture

1X 2N274

b. Plug-Half of the Fracture

FIGURE 2. FRACTURE-SURFACE APPEARANCE OF THE VALVE-STEM FAILURE

side of the stem is identified by Arrow 2 in both Figures 2a and 2b. The curved boundaries of the thumbnail patterns and other marks on the fracture surface with similar curvatures are beach marks, also called clamshell, conchoidal, or arrest marks. The small arrows in Figure 2 identify two different beach marks. Generally, beach marks having the same curvature are centered around a common point that corresponds to the fatigue-crack origin. Beach marks usually develop as a result of changes in loading or frequency, or by oxidation of the fracture surface during periods of crack arrest from intermittent service of the part. Thus, the beach marks and thumbnail patterns observed on the fracture surface indicated that a primary fatigue crack initiated within the circled area identified in Figures 2a and 2b and the secondary fatigue cracked initiated within a similar region on the side of the stem opposite the primary fatigue crack. However, the specific crack origins could not be identified by visual and stereomicroscopic examinations.

The two fatigue cracks propagated in opposite directions. The primary fatigue crack propagated much farther across the diameter of the stem, as indicated by the location of the beach mark identified by the small arrow in Figure 2a, than did the secondary fatigue crack. The final fracture zone between the two opposing fatigue cracks was not identified. The zone was apparently very small, since the tips of the two cracks apparently were very close to each other when final fracture of the remaining section occurred.

The presence of two opposing fatigue cracks indicated that the cracks initiated from reverse-bending stresses. The magnitude of those stresses were indicated by the very small final-fracture zone to be nominally very low. Either the primary crack initiated and propagated under somewhat higher bending stresses than did the secondary crack, or the primary crack initiated earlier and propagated for a longer time than did the secondary crack.

A visual examination of the plug revealed six areas of wear about 1 1/4-inch square on the cylindrical surface of the lower plug. The wear areas were spaced at 60-degree intervals around the plug. The worn surfaces had the appearance of a highly-polished, peened or hammered

surface. Relative to the fracture surface features, two opposing wear areas were in alignment with the origin regions of the two opposing fatigue-cracks.

Measurements of the depths of wear on the lower plug were made using a dial-displacement gage while the plug was rotated 360 degrees in a lathe. The gage was adjusted to zero at a location on the cylindrical surface midway between two wear areas. The results of the depth measurements are recorded in Figure 3. Two adjacent wear areas were worn to depths of 0.020 and 0.024 inch, respectively. The depths of the remaining wear areas were 0.006 inch or less. The primary fatigue-crack-origin region was found to be aligned with, and on the same side of the valve stem, as was the area, Wear-Location 1 in Figure 3, that was worn to a depth of 0.020 inch. The secondary fatigue-crack origin was on the same side and aligned with the wear area identified in Figure 3 as Wear-Location 2.

Scanning-Electron-Microscopic Examinations. The surface of the stem-half of the fracture was examined in the scanning electron microscope (SEM) in the as-received condition and after removal of corrosion products by electrochemical cleaning techniques. The SEM examinations were concentrated in the region of the origin of the primary fatigue crack. A SEM micrograph of the origin region before cleaning is shown in Figure 4.

The origin region exhibited considerable mechanical damage, which is evident as smooth, dark-gray areas in Figure 4a. Figure 4a also shows, in the region of letter T, the portion of the thumbnail pattern nearest to the origin of the fatigue crack. Fracture ridges within the thumbnail appeared to radiate outward from the approximate location in Figure 4a of the letter X, which was subsurface and within the fillet weld. The point or site from which fracture ridges diverge usually is the location of the crack origin. No evidence of a crack origin was observed in the immediate region identified by the letter X. The region exhibited much mechanical damage which may have obliterated evidence of an origin.

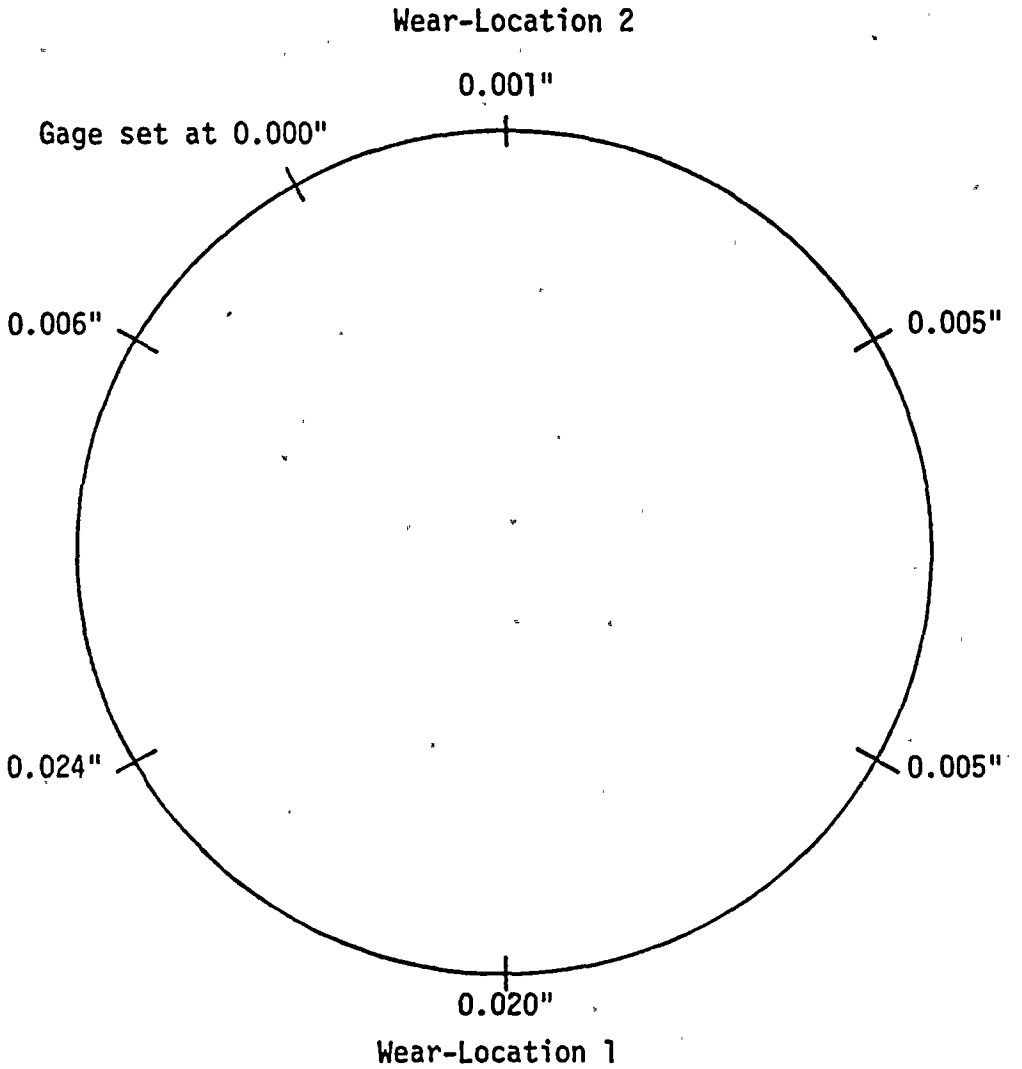

FIGURE 3. SKETCH SHOWING THE DEPTH OF WEAR AT THE 60-DEGREE WEAR LOCATIONS ON THE LOWER PLUG

The primary fatigue-crack origin was approximately in alignment with, and on the same side of the stem, as was the side of the lower plug at Wear-Location 1 in the sketch. Similarly, the secondary fatigue-crack origin was in alignment with Wear-Location 2 in the sketch.

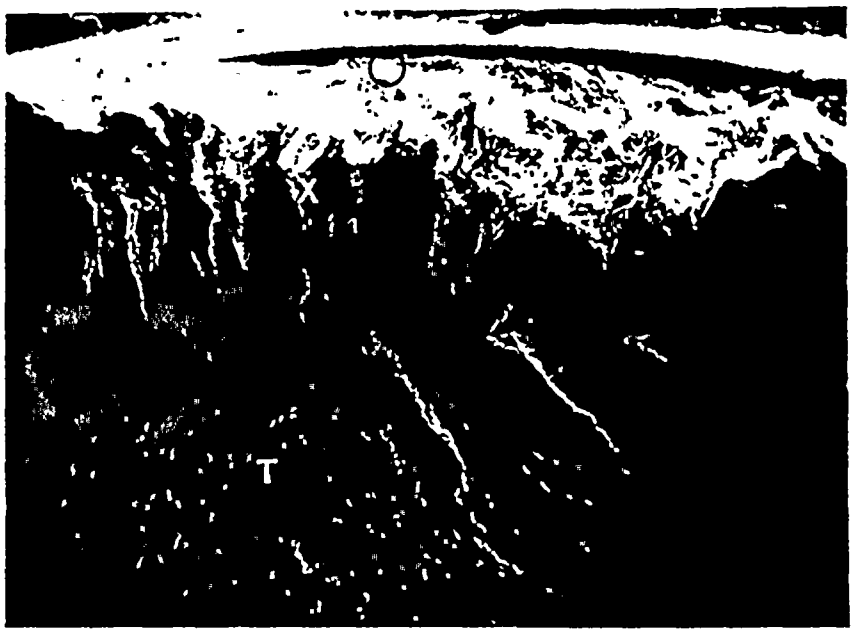

14X 76028

a. Origin Region of the Primary Fatigue Crack

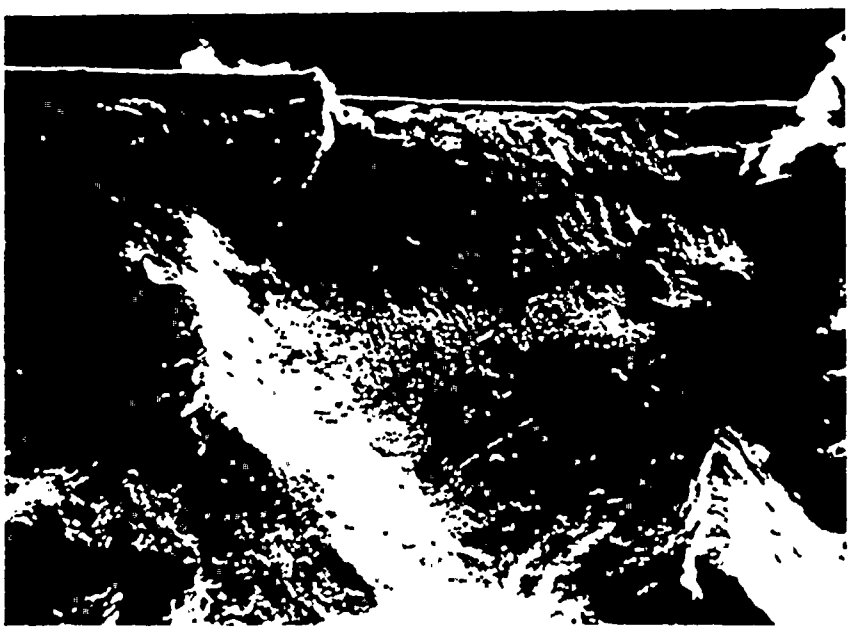

500X 76030

b. Circled Area in (a) Above at a Higher Magnification

FIGURE 4. FRACTURE FEATURES OBSERVED IN THE CRACK-ORIGIN REGION BY SCANNING ELECTRON MICROSCOPY BEFORE CLEANING

2500X 76029A

c. Apparent Fatigue Striations Observed at a Higher Magnification Within the Encircled Area in Figure 4b
(The arrow indicates the direction of crack propagation.)

FIGURE 4. CONTINUED

Figure 4b shows the fracture surface in weld metal within the circled area in Figure 4a. The circled area in Figure 4b is shown at a higher magnification in Figure 4c. Striations, which appear to be fatigue striations, are evident in Figure 4c. The curvature of the striations indicated that the direction of crack propagation was in the direction of the arrow in Figure 4c, which was outward to the surface of the fillet weld; that direction of crack propagation also suggested that the crack origin was subsurface and in the general vicinity of Location X in Figure 4a.

An area of corrosion products observed on the fracture surface within the primary thumbnail pattern is shown in Figure 5. Those corrosion products were characterized by a cracked appearance and the presence of chlorine that was detected by EDS microprobe analysis. Very few areas were observed that exhibited this type of corrosion products. Other corroded areas did not exhibit the cracked appearance nor was the presence of chlorine detected in those areas.

The cleaned surface of the fracture in the primary origin region is shown in Figure 6. Figure 6a is the same area as that in Figure 4a and shows essentially the same macroscopic features. No specific crack initiation site was identified within the suspected origin region. However, fatigue striations, other than those shown in Figure 4c, were observed. Those striations are shown in Figures 6c and 6d, which are higher magnification fractographs of the encircled region identified in Figure 6b. The curvature of the striations, like those shown in Figure 4c, indicated that crack propagation proceeded outward to the surface of the fillet weld from an initiation site that was subsurface and apparently within weld metal.

Typical features observed on the surface of the fracture across the valve stem are shown in Figure 7. Those features included very fine fatigue striations; examples are evident between pairs of arrow heads shown in Figure 7b.

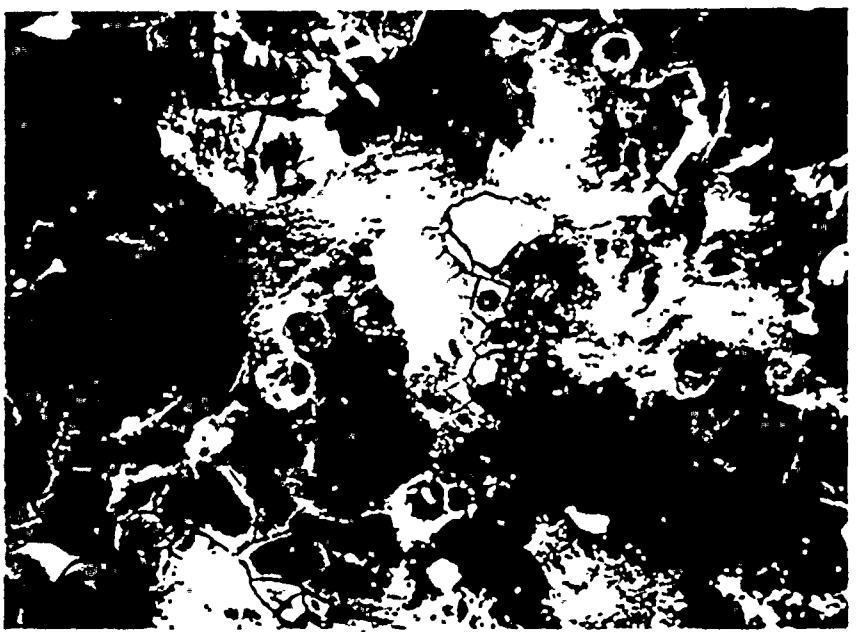

500X 76035

FIGURE 5. CORROSION PRODUCTS WHICH CONTAINED CHLORINE ON THE FRACTURE SURFACE

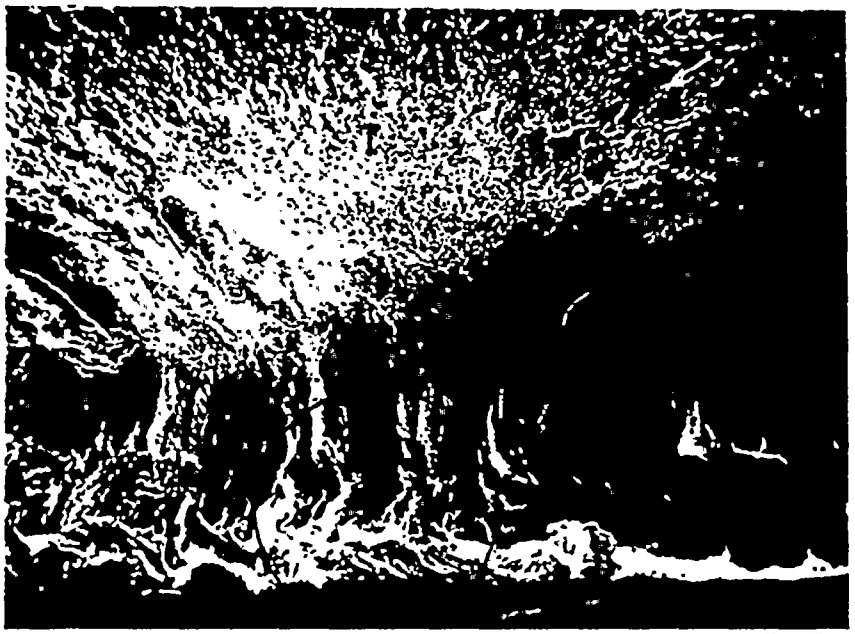

15X 76055

a. Origin Region of the Primary Fatigue Crack (Same area as that shown in Figure 4a.)

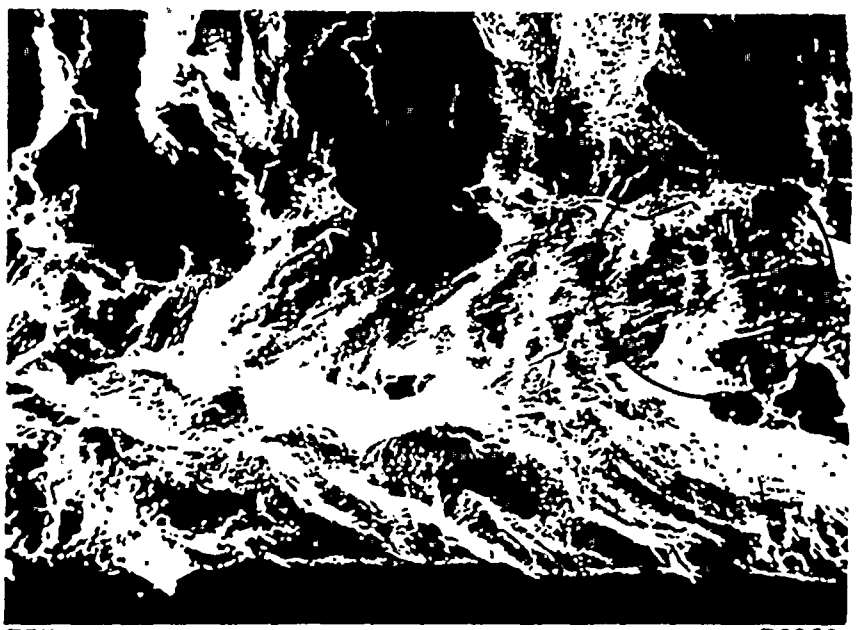

75X 76060

b. Circled Area in (a) Above at a Higher Magnification

FIGURE 6. FRACTURE FEATURES OBSERVED IN THE CRACK-ORIGIN REGION BY SCANNING ELECTRON MICROSCOPY AFTER CLEANING

250X 76057

c. Circled Area in (b) at a Higher Magnification Showing Apparent Fatigue Striations

(The arrow indicates the direction of crack propagation.)

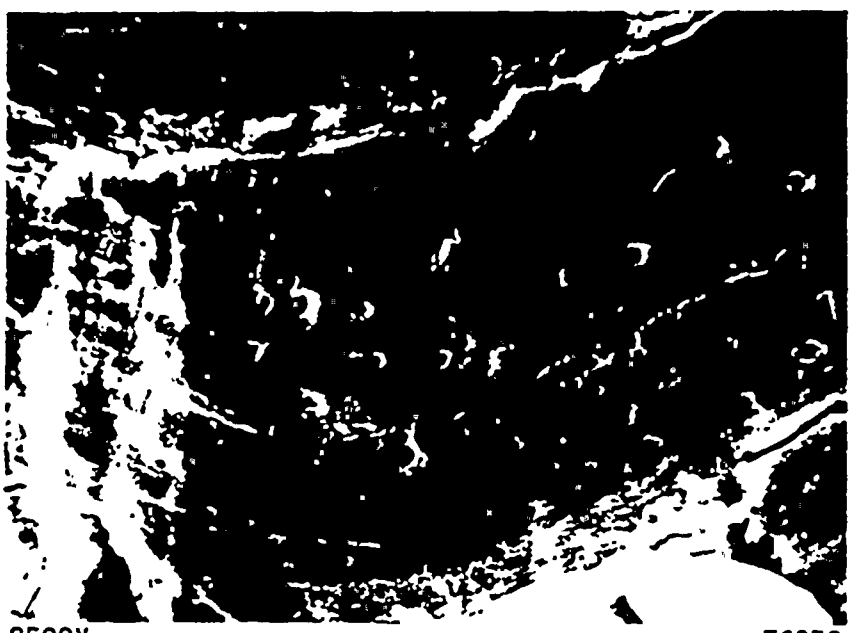

2500X 76058

d. Higher Magnification of Apparent Fatigue Striations Shown in (c) Above

FIGURE 6. CONTINUED

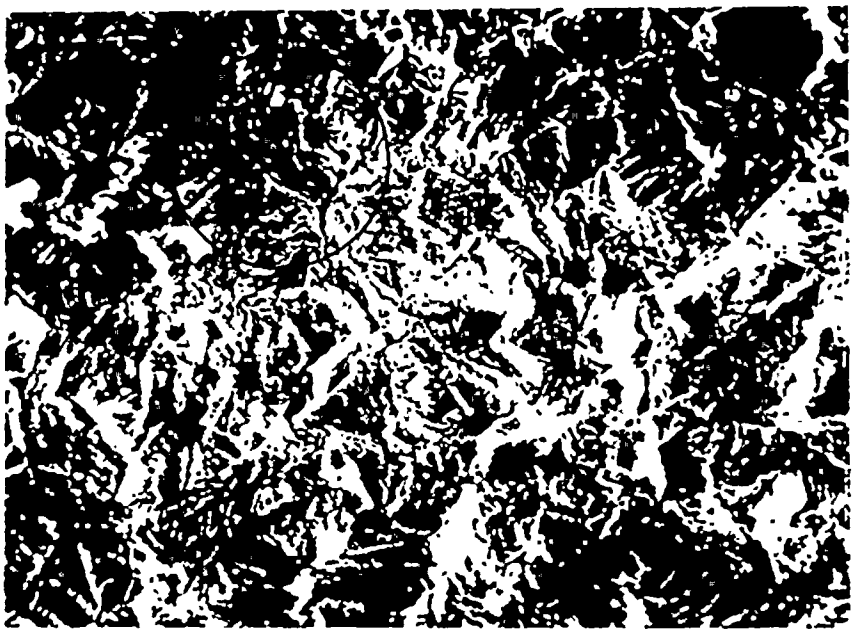

500X 76061

a. An Area Within the Thumbnail Pattern in the General Region of Letter T in Figure 6a

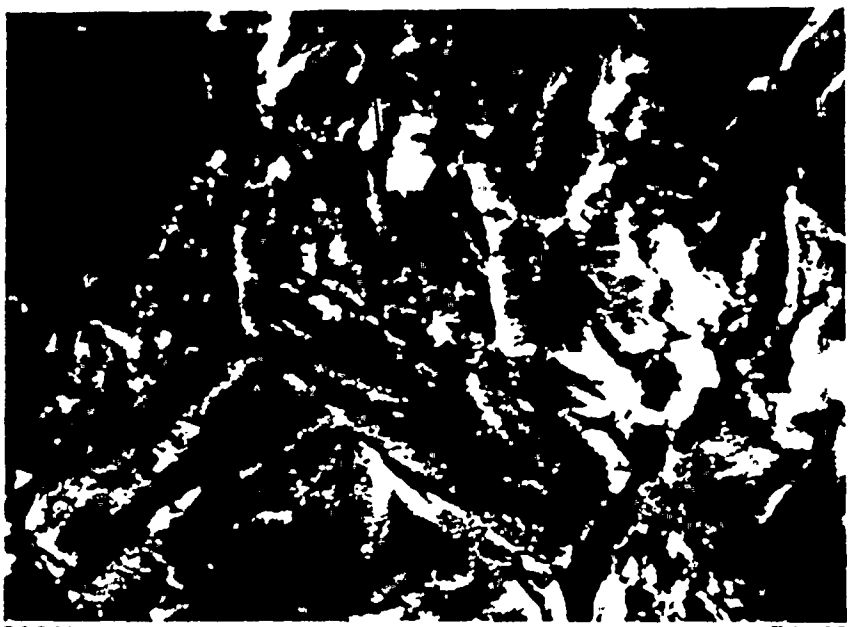

2000X 76062

b. Very Fine Fatigue Striations (between pairs of arrowheads) Within the Area Encircled in (a) Above

FIGURE 7. TYPICAL FEATURES OBSERVED ON THE FRACTURE SURFACE IN THE VALVE STEM

Metallographic Examinations

A cross section of the matched fracture halves was prepared metallographically for examination. The cross section intersected the general region of the crack origin that was indicated by the primary thumbnail pattern on the fracture surface. The metallographic specimen was ground, polished, etched and examined successively seven times at increments of 5 to 10 mils, in an attempt to intersect and identify a surface or subsurface flaw, or other microstructural abnormality from which the primary fatigue crack initiated. No crack initiator was identified during the examinations of those seven serial sections.

The fracture was observed in the metallographic sections to be transgranular through the weld metal and across the stem. The microstructure of the weld metal was typical of the microstructure of Type 316 stainless steel weld metal in the as-welded condition. The microstructure of the stem was typical of the microstructure of wrought and annealed Type 316 stainless steel. No evidence of sensitization in the microstructure of the weld-heat-affected zone of the stem was observed. A photomacrograph of one of the seven serial sections is shown in Figure 8a. The primary fatigue crack was located on the side of the stem identified by the arrow in Figure 8a; a portion of the fillet weld and crack is shown in Figure 8b at a higher magnification.

Discussion

The results of the fractographic examinations indicated that the mode of crack propagation was primarily fatigue. The mode of crack initiation, although not observed on the fracture surface since a specific site of crack initiation was not identified, apparently was fatigue also. The macroscopic features of the primary fatigue-thumbnail pattern and the microscopic fatigue striations, which were observed, indicated that the general vicinity of the initiation site was subsurface near the root of the weld. The nature of a crack initiator at that location would most likely be that of a weld flaw, such as a hot crack or weld-metal pore. Flaws of that nature are frequently stress-raisers

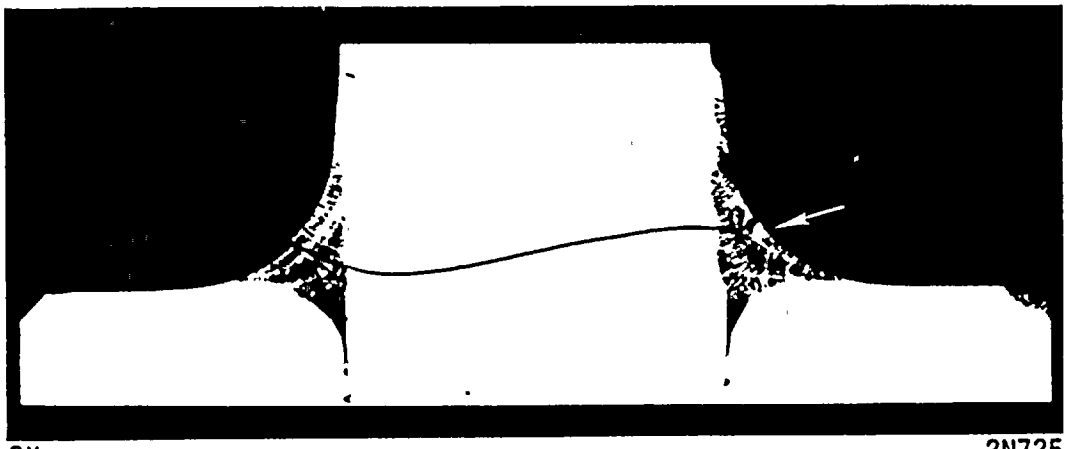

2X 2N725

a. Cross Section of Matched Fracture Halves Through the Primary Origin Region at the Fillet Weld Indicated by the Arrow

25X 2N726

b. Higher Magnification of the Fillet Weld Indicated by the Arrow in (a) Above

FIGURE 8. A METALLOGRAPHIC CROSS SECTION THROUGH THE PRIMARY FATIGUE-CRACK-ORIGIN REGION

about which the magnitude of the resultant stress concentration can exceed the fatigue strength of the metal. Hence, a fatigue crack initiates in the adjacent metal and propagates.

The stresses involved in the initiation and propagation of the fatigue failure were indicated to be reverse-bending stresses. The presence of residual stresses induced by welding would be additive to the service stresses. The bending stresses apparently developed during wear at the lower plug. As the wear, particularly on one side of the lower plug, progressed to greater depths, the clearance between the body of the valve and the lower plug increased, and the welded joint between the plug and stem was subjected to a bending moment. The bending stresses would be expected to increase as the depth of wear on the lower plug increased. Ultimately, the magnitude of those stresses plus residual-welding stresses, multiplied by a stress-concentration factor of an internal flaw, if present, apparently was sufficient to start a fatigue crack.

Conclusions

The results of the metallurgical investigation of the plug and valve stem failure led to the following conclusions:

(1) The mode of crack propagation was fatigue.

(2) A specific crack origin was not identified, but the location of the origin appeared to be subsurface within the fillet weld metal.

(3) Fatigue crack propagation was induced principally by reverse bending stresses.

(4) Bending stresses apparently developed as a result of wear on the lower plug. The bending stresses probably increased as the depth of wear increased.

(5) The microstructures of the weld metal and stem were normal.

(6) The chemical compositions of the weld metal and stem were within the composition limits of Type 316 stainless steel. The chemical composition of the plug was apparently that of a cast stainless steel alloy, CF8M.

Recommendations

The results of the investigation indicated that, to prevent a failure of this type in the plug and valve stem, the stress concentration in the fillet weld and the bending stresses should be minimized. Two recommendations are suggested to accomplish this.

(1) Increase the diameter of the stem at the welded joint and use a streamline, elliptical or parabolic form of fillet instead of a constant radius (circular fillet).

(2) Consider a change of design and/or material for the plug to reduce the amount of wear that occurs on the lower end of the plug.

PART TWO: STAINLESS STEEL WELD METAL FROM FEEDWATER PIPE

Introduction

The failure of the stainless steel welded pipe occurred in a circumferential weld between a carbon steel pipe and a 5 percent chromium steel pipe, which were reported to be about 8 to 10 inches in diameter. The welded pipe was from the suction side of the feedwater pump and contained feedwater at 316 F and an internal pressure of about 170 psig. The pipe was reported to have been considerably repair welded at least 18 years ago. The repair welding process was not reported to Battelle. The failure was a crack in the weld metal which eventually propagated through the joint and allowed feedwater to leak into insulation on the outside of the pipe. The type of insulation was not reported to Battelle. A boat sample containing a portion of the crack was furnished to Battelle for a metallurgical investigation of the cause of the crack.

Summary

A crack contained in a weld-metal boat sample removed from a circumferential austenitic stainless steel weld was investigated to determine the most probable cause of the failure. The investigation involved primarily a chemical analysis of the weld metal, fractographic studies of the crack surface, and metallographic studies of a cross section of the crack.

The results of the investigation indicated that the crack most likely was caused by intergranular stress-corrosion cracking (IGSSC). The weld metal was found to be sensitized and, thereby, was susceptible to IGSSC. The stresses which assisted intergranular corrosion were believed to be a combination of residual welding stresses and applied service stresses.

A recommendation was made to eliminate sensitization by using a stabilized austenitic welding electrode, such as E347, and by avoiding

prolonged heating or slow cooling of the weld metal in the temperature range of 1000-1500 F.

Results of Laboratory Examinations

Chemical Analysis

A chemical analysis of the weld metal from the boat sample was obtained using emission spectrographic analytical techniques. The results of the chemical analysis are presented in Table 3. Included in Table 3 are the composition limits for an austenitic stainless steel electrode, EX310T-X, which is used for flux cored arc welding (FCAW). An austenitic stainless steel electrode, E310, which is used for shielded metal are welding (SMAW) has composition limits similar to those of EX 310T-X. The results of the chemical analysis of the weld metal from the boat sample indicated that the welding electrode used for repair welding was most likely the Type 310 stainless steel electrode used for either FCAW or SMAW.

Fractographic Examinations

The boat sample containing the crack was sectioned lengthwise in half. The portion of the crack in one half of the boat sample was broken open in the laboratory to expose the fracture surface for fractographic examinations. Those examinations were made in the scanning electron microscope (SEM). The cut face of the other half of the boat sample, which contained the remainder of the crack, was mounted and prepared metallographically for examination.

SEM examinations of the fracture surface were performed before and after cleaning the surface since corrosion products and discolorations were evident. The evidence of corrosion and discolorations was most prominent on the surface of the fracture nearest the inside surface of the welded pipe and the evidence diminished across the fracture surface toward the outside surface.

TABLE 3. EMISSION SPECTROGRAPHIC ANALYSIS OF THE CHEMICAL COMPOSITION OF THE WELD METAL FROM THE BOAT SAMPLE

Element	Content, weight percent	
	Boat Sample, weld metal	FCAW Electrode, EX310T-X[(a)]
Carbon	0.12	0.20
Manganese	1.61	1.0-2.5
Phosphorus	0.022	0.03
Sulfur	0.010	0.03
Silicon	0.50	1.0
Copper	0.008	0.5
Tin	0.012	
Nickel	19.7	20-22.5
Chromium	26.5	25-28
Molybdenum	0.06	0.5
Aluminum	0.005	
Vanadium	0.05	
Niobium	0.01	
Zirconium	0.002	
Titanium	0.015	
Boron	0.0002	
Calcium	0.0032	
Cobalt	0.08	
Tungsten	0.00	

(a) Composition limits for a Type 310 stainless steel electrode used for flux cored arc welding (FCAW). ASM Metals Handbook, Vol. 6, Ninth Edition.

A low-magnification SEM micrograph of the fracture surface before cleaning is shown in Figure 9. Crack propagation appeared to be along columnar, weld-metal grain boundaries which gave a "woody" appearance to the fracture surface. EDS microprobe analyses of several areas on the uncleaned fracture surface did not detect the presence of any unusual elements, such as chlorine or sulfur that might indicate a specific ionic specie was responsible for the corrosion attacks.

A typical area of the fracture surface after cleaning is shown in Figure 10. Most of the fracture surface was relatively smooth, which is typical of an intergranular mode of crack propagation along columnar grains of the weld metal. However, small particles, some of which are indicated by arrows in Figure 10, were observed in the smooth intergranular surfaces of the fracture. Those particles indicated the presence of an intergranular phase.

Metallographic Examinations

The portion of the metallographic cross section of the boat sample which contained the crack through weld metal is shown in Figure 11a. Intergranular fracture along the columnar grain boundaries of the weld metal is evident in Figure 11a. Figure 11b shows a portion of the intergranular fracture at the outside surface of the weld in a plane different from that shown in Figure 11a. In addition to the intergranular fracture, Figure 11b shows two small transgranular cracks in the outside surface of the weld; those cracks are identified in Figure 11b by arrows. Four other small transgranular cracks were observed elsewhere in the outside surface of the weld. One of the other four cracks is shown in Figure 12. All of the small transgranular cracks exhibited crack-branching; the appearance of the cracks was typical of transgranular stress-corrosion cracking in stainless steel. However, none of the cracks appeared to be associated with, or related to, the intergranular fracture through the weld metal.

The microstructure of the weld metal, revealed by etching the specimen with a solution consisting of 97 ml. conc. HCl, 3 ml. conc. HNO_3, and 1/2 g $CuCl_2$, exhibited the presence of an intergranular phase.

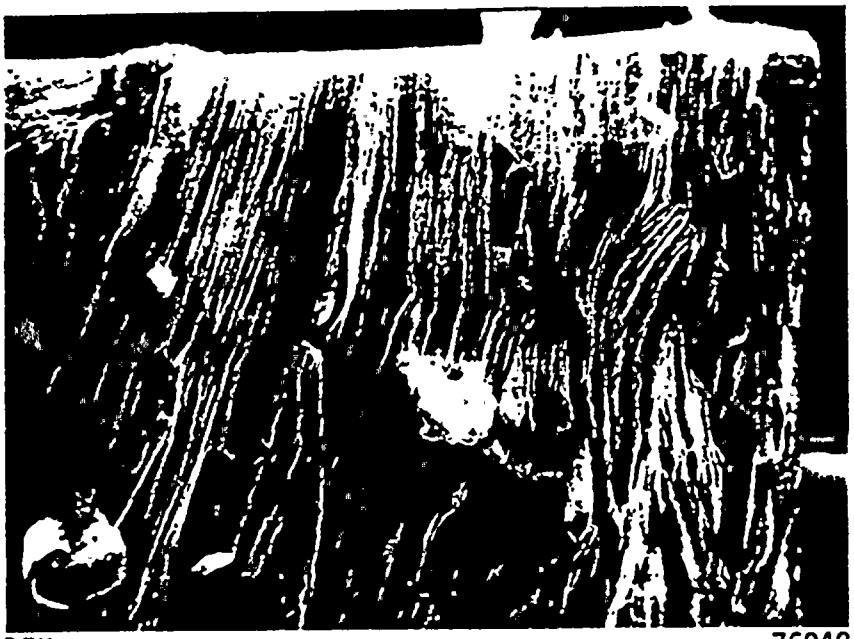

15X 76042

FIGURE 9. "WOODY" APPEARANCE OF THE SURFACE OF THE WELD-METAL CRACK IN THE BOAT SAMPLE

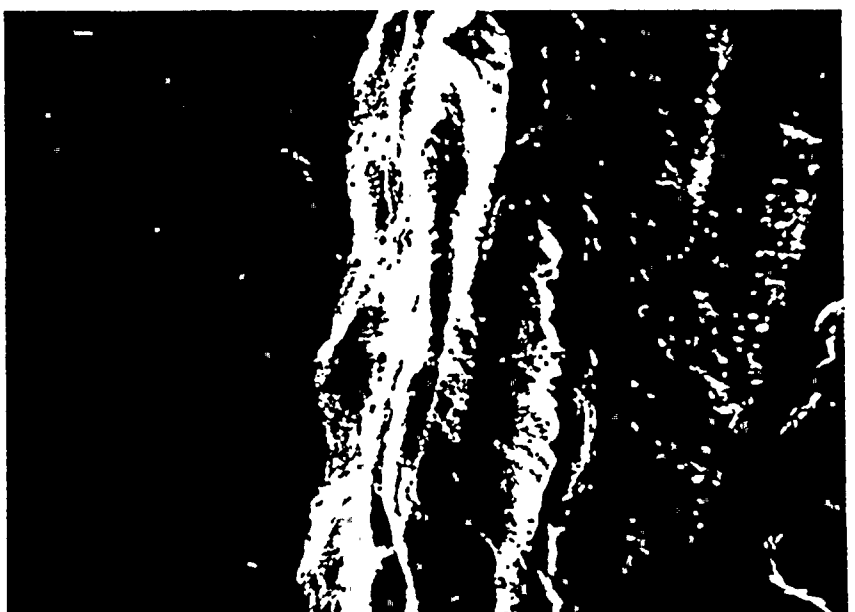

500X 76070

FIGURE 10. TYPICAL AREA OF THE CRACK SURFACE AFTER CLEANING

Arrows identify some of the intergranular particles.

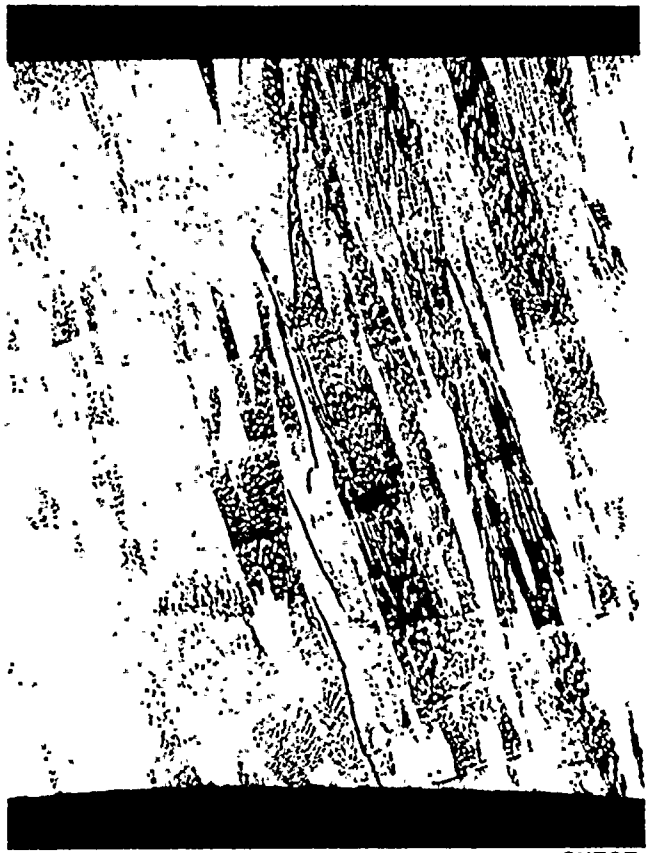

a. Section Completely Across the Weld (Boat Sample)

b. Cross Section of the Weld at the Outside Surface (arrows identify secondary transgranular cracks)

FIGURE 11. METALLOGRAPHIC CROSS SECTION OF THE BOAT SAMPLE SHOWING THE NATURE OF THE INTERGRANULAR FRACTURE THROUGH WELD METAL

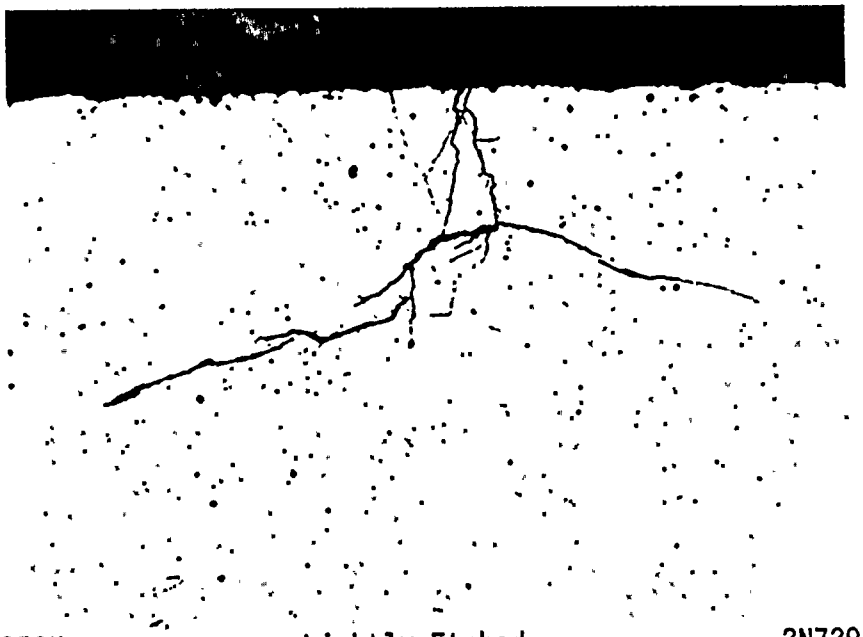

250X Lightly Etched 2N729

FIGURE 12. ONE OF THE SMALL TRANSGRANULAR STRESS-CORROSION CRACKS OBSERVED IN THE OUTSIDE SURFACE OF THE WELD METAL

Figures 13a and 13b show examples of the intergranular phase in two areas of the weld metal where the phase was displayed most prominently. The phase was evident in virtually all of the weld-metal grain boundaries observed in the metallographic specimen. Occasionally, the phase exhibited a lamellar morphology, as shown in Figure 13b.

The circled area shown in Figure 13b was selected for the wavelength-dispersive (WDS) analysis. WDS is capable of detecting the presence of elements of atomic Number 5, boron, and higher. The intergranular phase was identified as a carbide by X-ray WDS microprobe analysis in conjunction with the scanning electron microscope. A SEM micrograph (secondary-electron image) of the area is shown in Figure 13c at a higher magnification. An X-ray distribution map of carbon in the area is shown in Figure 13d. The X-ray distribution map reveals a concentration (high-density of white dots in the X-ray distribution map) of carbon in the intergranular phase. A slight concentration of chromium and depletion of iron relative to the concentration of those elements in the surrounding weld-metal matrix also were detected in the phase by the WDS X-ray counts for those elements. Thus, the intergranular phase was most likely an iron-chromium carbide.

Discussion

The most significant results of the laboratory examinations were (1) the presence of discolorations and corrosion on the fracture surface which was more evident toward the inside surface than toward the outside surface of the pipe, (2) a fracture mode identified as intergranular, and (3) the presence of an intergranular carbide phase. The distribution over the fracture surface of corrosion and discolorations indicated that the failure most likely started on the inside surface of the circumferential pipe weld. The surface of the earlier stages of crack propagation were apparently exposed to the corrosive environment for longer periods of time. The presence of intergranular carbides in the weld metal constituted a sensitized condition of the weld metal. Stainless steels derive their resistance to corrosion principally from the presence of chromium. The formation of intergranular iron-chromium

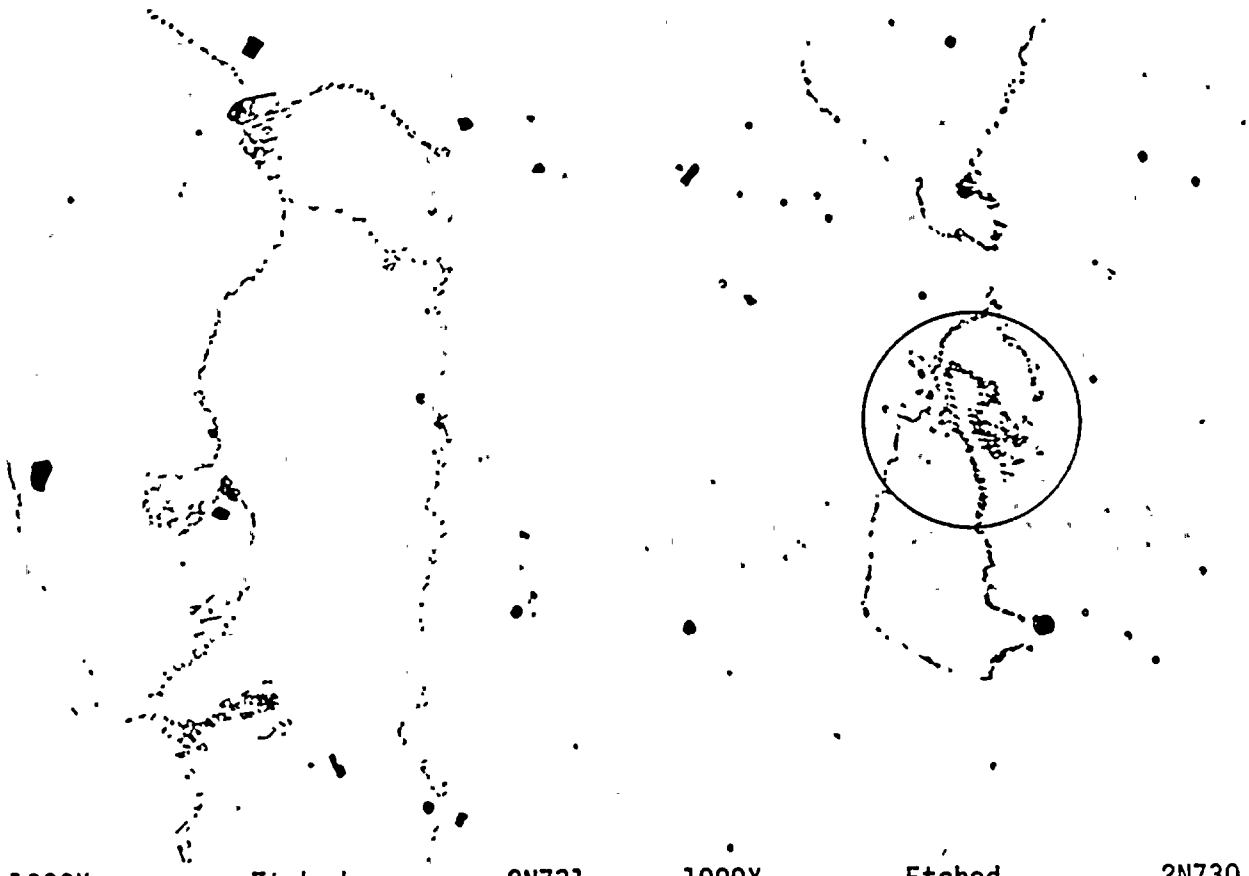

FIGURE 13. EXAMPLES OF THE INTERGRANULAR CARBIDE PHASE OBSERVED IN THE WELD-METAL GRAIN BOUNDARIES

3600X Etched P989

c. Secondary Electron Image of the Area Encircled in (b) at a Higher Magnification

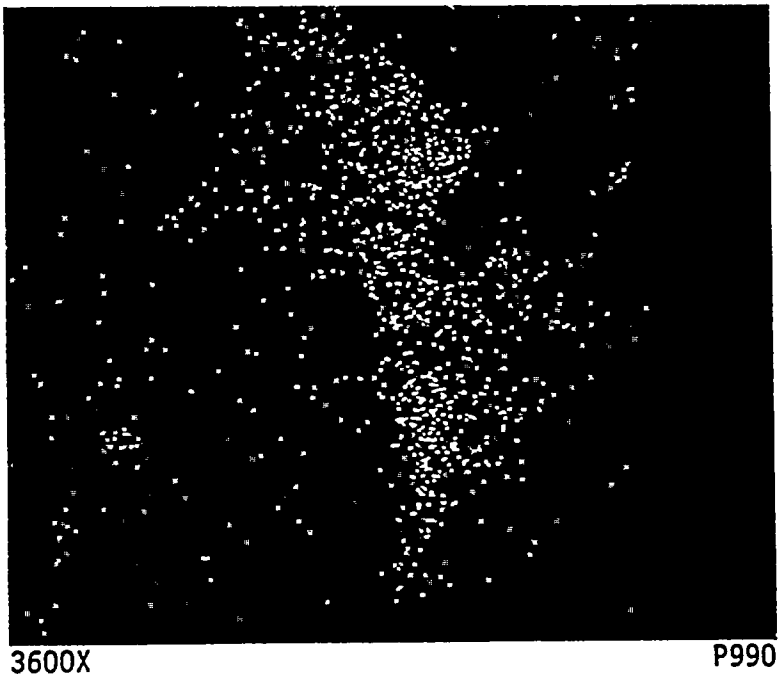

3600X P990

d. X-ray Distribution Map of Carbon in the Area Shown in (c) Above

FIGURE 13. CONTINUED

and/or chromium carbides (sensitization) depletes the areas adjacent to the grain boundaries of chromium and those areas become susceptible to intergranular corrosion attack. Stainless steels stabilized with additions of niobium (columbium) or titanium, which combine with carbon and prevent chromium carbide precipitation, do not normally become sensitized. The composition of the weld metal indicated that unstabilized stainless steel welding electrodes were used for the repair weld.

Unstabilized stainless steel becomes sensitized if heated to temperatures in the range 1000 to 1550 F, or if cooled slowly through that temperature range. High heat input and low travel speeds induce sensitization in stainless steel weld metal. Welding processes that have a high potential for carburizing stainless steel, such as dry fuel-gas welding, which also has a high heat input, increases the sensitization of weld metal.

Intergranular corrosion of sensitized material may occur with or without stress. The former failure mode is often referred to as intergranular stress-corrosion cracking (IGSCC). IGSCC occurs most often in corrosive environments of polythionic acid solution or of high-temperature oxygenated water. The specific corrosive element which apparently led to the intergranular attack of the stainless steel weld metal, was not identified by the laboratory examination performed. However, oxygenated feedwaters are known to cause ISCC. Although the welded pipe was reported to be under a relative low stress, residual stresses in weldments are often sufficient to sustain either SCC or IGSCC. Conventional transgranular SCC, such as the secondary SCC observed on the outside surface of the weld metal, usually occurs in chloride or caustic solutions. The observed transgranular SCC probably occurred after leakage of the pipe. The moisture on the outside surface of the weld metal may have leached chlorine from the insulation which, combined with residual and/or applied stresses, led to the observed transgranular SCC.

Conclusions

The results of the metallurgical investigation led to the following conclusions:

(1) The failure of the weld metal was most likely caused by intergranular stress-corrosion cracking (IGSCC).
(2) The weld metal was sensitized and thereby was susceptible to IGSCC.
(3) The corrosive environment was not identified. The environment might have been high-temperature oxygenated feedwater.

Recommendations

In order to eliminate sensitization and the subsequent potential IGSCC in austenitic stainless steel weld metal, it is recommended that a stabilized stainless steel welding electrode, such as E347, be used, and that prolonged heating or slow cooling of the weld metal through the temperature range of 1000 to 1550 F be avoided.

RESEARCH REPORT

on

METALLURGICAL INVESTIGATIONS OF TWO TWO FAILED COMPONENTS

PART ONE: PLUG AND VALVE STEM, PART NO. FW-13A-FCV

PART TWO: STAINLESS STEEL WELD METAL FROM FEEDWATER PIPE

to

NIAGARA MOHAWK POWER CORPORATION

February 17, 1988

by

R. D. Buchheit and T. P. Groeneveld

BATTELLE
Columbus Division
505 King Avenue
Columbus, Ohio 43201-2693

APPENDIX E

Battelle
Columbus Division
505 King Avenue
Columbus, Ohio 43201-2693
Telephone (614) 424-6424
Telex 24-5454

February 17, 1988

Mr. Lee Klosowski
Niagara Mohawk Power Corporation
Salina Meadows
301 Plainfield Road
Syracuse NY 13212

Dear Mr. Klosowski:

Attached are two copies of a final report of Battelle's metallurgical investigation of two failures, (1) a fracture of a stem and plug, Part No. FW-13A-FCV, and (2) a cracked weld in pipe from the suction side of the feedwater pump, from the Nine Mile Point Unit #1 Nuclear Station, Lycoming, New York.

Briefly, the results of the investigation of the stem/plug failure indicated that the fracture of the stem at the fillet weld was caused by reverse-bending fatigue induced by wear on the surface of the lower plug. The results of the investigation of the cracked stainless steel weld metal in the feedwater pipe indicated that the failure was caused by intergranular-stress-corrosion-cracking, IGSCC, of sensitized weld-metal grain boundaries. Sensitization of the grain boundaries apparently occurred at the time the pipe was welded since austenitic stainless steel does not become sensitized at the service temperature, which was reported to be 316 F.

Mr. Robert Cushman (NMPC) requested today that the following information in regard to the stem/plug failure be included in this covering letter. The weight of the plug was approximately 61 pounds; the radius of the fillet weld at the threaded joint between the stem and the plug was about 0.4 inch.

Both investigations were very interesting and a pleasure to conduct. If any questions arise concerning the content of the report and/or the results obtained, please do not hesitate to call me at (614) 424-4049.

Very truly yours,

R. D. Buchheit
Principal Research Engineer
Physical Metallurgy Section

xc: Mr. T. W. Roman (2 copies)
Station Superitendent

Mr. F. A. Hawksley (covering letter only)

TABLE OF CONTENTS

LIST OF TABLES

LIST OF FIGURES

METALLURGICAL INVESTIGATIONS OF TWO FAILED COMPONENTS

by

R. D. Buchheit and T. P. Groeneveld

from

BATTELLE
Columbus Division

February 17, 1988 .

INTRODUCTION

Failures of two components occurred at the Nine Mile Point Unit No. 1 Nuclear Station of Niagara Mohawk Power Corporation (NMPC). At the request of NMPC, the Battelle Columbus Division conducted a metallurgical investigation of the failed components to determine, insofar as possible, the most probable cause of each failure.

One of the failures occurred in NMPC Part No. FW-13A-FCV. The part was a component of a feedwater flow-control valve. The other failure occurred in a stainless steel welded pipe joint from the suction side of the feedwater pump. This report consists of two parts which describe the details and results of the metallurgical investigation of each failure, respectively. Part One describes the investigation of the valve stem and plug, Part No. FW-13A-FCV; Part Two describes the investigation of welded feedwater pipe.

PART ONE: PLUG AND VALVE STEM, PART NO. FW-13A-FCV

Introduction

The failed component of NMPC Part No. FW-13A-FCV consisted of a plug and valve stem. The stem was threaded into one end of the plug and fillet-welded circumferentially to the plug at the threaded joint. A sketch of the plug/stem component within the body of the control valve is presented in Figure 1. The location of the failure is indicated in

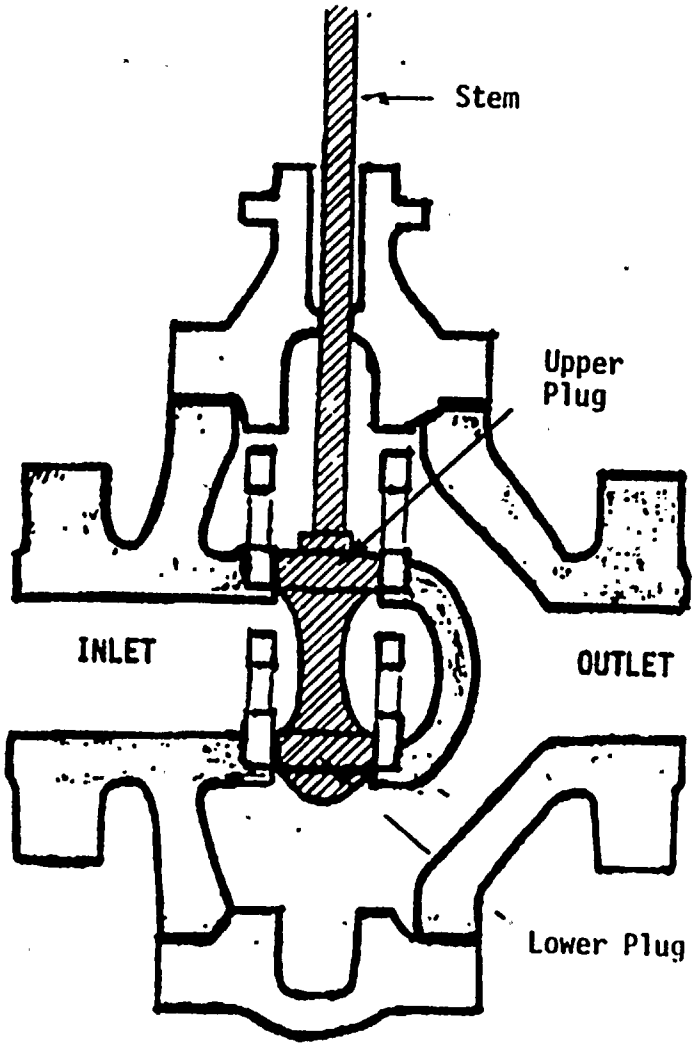

a. Stem/Plug in the Closed Position

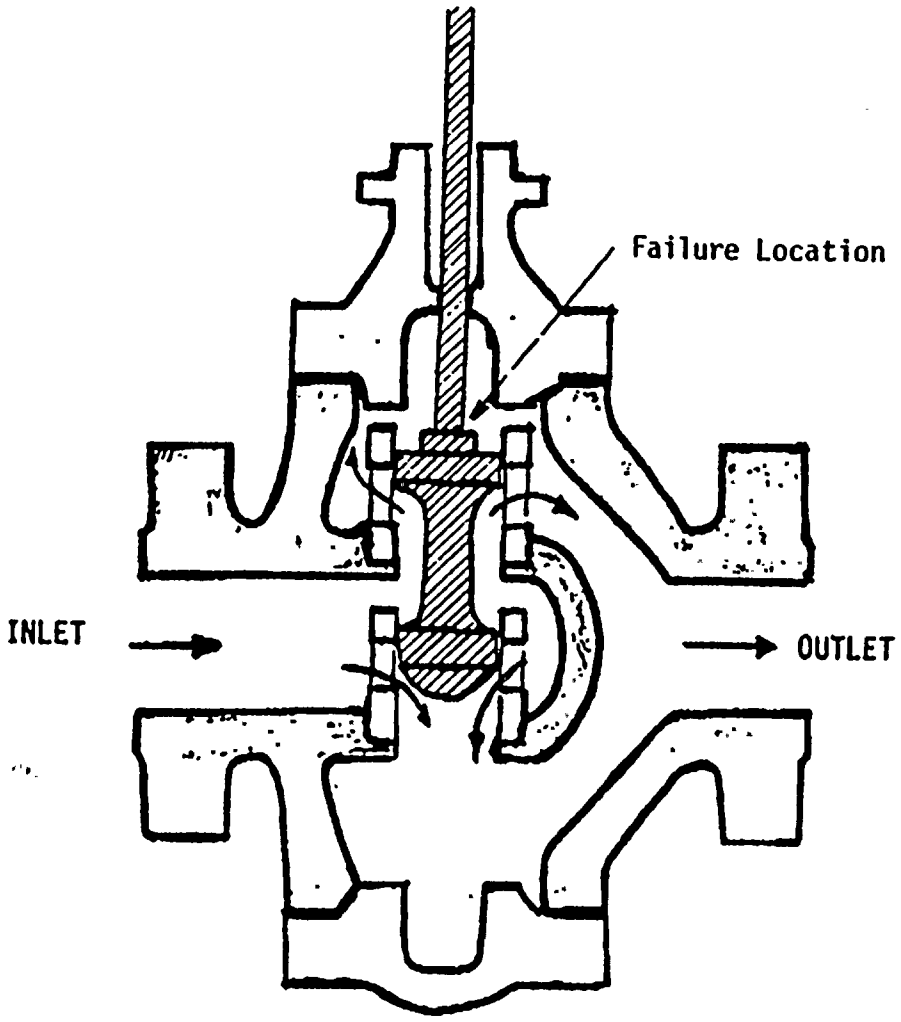

b. Stem/Plug in the Open Position

FIGURE 1. SKETCH OF THE FLOW-CONTROL VALVE SHOWING THE STEM/PLUG COMPONENT, PART NO. FW-13A-FCV (Cross-hatched area) Drawing supplied by NMPC

Figure 1b. The failure was a transverse fracture of the 1-inch-diameter stem through the fillet weld.

The plug was reported to be a stainless steel casting, and the stem and fillet weld-metal also were reported to be stainless steel; however, the type or grades of stainless steel were not reported. The valve controlled the flow of demineralized feedwater back to the reactor at 316 F under a pressure of 1278 psig. The service time of the valve was reported to be from June 1986 to December 1987; the valve operated continuously for 415 days during that period of time.

NMPC submitted the entire fractured stem and plug to Battelle for the metallurgical investigation of the failure.

Summary

A metallurgical investigation of a fracture at the fillet weld between a valve stem and plug (Part No. FW-13A-FCV) was performed to determine the most probable cause of the failure. The investigation involved primarily a chemical analysis of the weld metal, fractographic studies of the crack surface, and metallographic studies of cross sections traversing the cracked region.

The results of the investigation indicated that the crack was a reverse-bending fatigue fracture. A primary and a secondary fatigue crack initiated from opposite sides of the stem, respectively. The regions of the crack origins appeared to be subsurface in weld metal, but no specific initiation sites were identified. The bending stresses were believed to have developed in service as a result of wear on the lower plug. As the depth of the wear increased, the bending stresses probably intensified.

The chemical compositions of the stem and fillet weld indicated those materials to be Type 316 stainless steel. The microstructures of the stem and fillet-weld metal were typical of wrought and annealed Type 316SS, and of Type 316SS weld metal, respectively. The plug was indicated by its chemical composition and microstructure to be an austenitic stainless steel casting designated as cast alloy CF8M.

Recommendations to prevent such failures in the future are: (1) to increase the diameter of the stem and to use a streamline, elliptical, or parabolic form of fillet at the welded joint, and (2) to consider a change of design and/or material for the plug to provide better wear resistance of the lower end of the plug.

Results of Laboratory Examinations

Chemical Analyses

Chemical analyses of the plug, stem, and fillet weld metal were conducted. The chemical compositions of the plug and stem were determined using emission spectrographic analytical techniques; the compotion of the fillet weld-metal was determined using X-ray energy-dispersive (EDS) microprobe analytical techniques in conjunction with the scanning electron microscope. (EDS microprobe analyses can detect elements of atomic number 11, sodium, and higher. The concentrations of the elements detected by that technique are relative and semi-quantitative.) The weld metal was analyzed by EDS because the amount of weld metal required for other analytical techniques was not readily available.

The results of the chemical analyses are presented in Tables 1 and 2. Included in Table 1 are the composition limits for Type 316 stainless steel and cast CF8M stainless steel for comparison with the chemical compositions obtained from the stem and plug, respectively. The composition of the stem satisfied the composition limits of Type 316 stainless steel. Except for the chromium content, the composition of the plug appeared to be more representative of the composition of CF8M, than of the composition of any other cast stainless steel.

As shown in Table 2, the principal elements detected in three areas of the fillet weld metal by EDS were iron, chromium, nickel, and molybdenum. Except for the relative concentration of molybdenum in Area 3, the relative concentrations of those elements were within the composition limits, which are included in Table 2, of AWS E316 stainless steel welding electrode.

TABLE 1. EMISSION SPECTROGRAPHIC ANALYSES OF THE CHEMICAL COMPOSITIONS OF THE STEM AND PLUG

Element	Content, weight percent			
	Stem	316SS[a]	Plug	CF8M[b]
Carbon	0.07	0.08 max	0.06	0.08 max
Manganese	1.71	2.00 max	0.36	1.5 max
Phosphorus	0.034	0.045 max	0.027	0.04 max
Sulfur	0.027	0.03 max	0.023	0.04 max
Silicon	0.59	1.00 max	1.30	2.0 max
Copper	0.25		0.10	
Tin	0.011		0.001	
Nickel	12.1	10-14	9.3	9-12
Chromium	17.8	16-18	16.6	18-21
Molybdenum	2.2	2-3	2.2	2-3
Aluminum	0.000		0.001	
Vanadium	0.05		0.05	
Niobium	0.01		0.006	
Zirconium	0.003		0.004	
Titanium	0.005		0.004	
Boron	0.0004		0.0001	
Calcium	0.0015		0.0012	
Cobalt	0.21		0.071	
Tungsten	0.00		0.00	

(a) Composition limits for wrought Type 316 stainless steel.

(b) Composition limits for cast CF8M stainless steel.

TABLE 2. X-RAY ENERGY-DISPERSIVE MICROPROBE ANALYSIS OF THE FILLET WELD METAL

Element Detected	Relative Concentration, weight percent			
	Area 1	Area 2	Area 3	AWS[(a)] E316
Iron	66.1	66.2	67.2	Bal.
Silicon	0.7	0.6	0.4	0.90 max
Nickel	13.3	13.1	13.1	11.0-14.0
Chromium	17.6	17.7	17.6	17.0-20.0
Molybdenum	2.3	2.4	1.7	2.0-3.0

(a) Composition limits for AWS E316 stainless steel welding electrode.

Therefore, the fillet weld metal was most likely a Type 316 stainless steel.

Fractographic Examinations

Visual and Low-Magnification Stereomicroscopic Examinations.

The stem, plug, and the opposing halves of the fracture surface were examined visually and at low magnifications (7 to 30x) using an optical stereomicroscope.

The macroscopic appearance of each half of the fracture surface is shown in Figure 2. The photomacrographs in Figure 2 are oriented so that the stem-half of the fracture (Figure 2a) matches the plug-half of the fracture (Figure 2b) by folding Figure 2a down on top of Figure 2b.

Although macroscopic fracture features on the left side of the fracture surfaces, as shown in Figure 2, and at many other regions around the periphery of the fracture surface were obliterated by mechanical damage, some fracture features, which were characteristic of fatigue-crack propagation, were evident in the remainder of the fracture surface. Those features were two thumbnail patterns on opposite sides of the stem and a few beach marks. The primary, or larger, thumbnail region is identified by Arrow 1 and the smaller thumbnail region on the opposite

1X 2N723

a. Stem-Half of the Fracture

1X 2N274

b. Plug-Half of the Fracture

FIGURE 2. FRACTURE-SURFACE APPEARANCE OF THE VALVE-STEM FAILURE

side of the stem is identified by Arrow 2 in both Figures 2a and 2b. The curved boundaries of the thumbnail patterns and other marks on the fracture surface with similar curvatures are beach marks, also called clamshell, conchoidal, or arrest marks. The small arrows in Figure 2 identify two different beach marks. Generally, beach marks having the same curvature are centered around a common point that corresponds to the fatigue-crack origin. Beach marks usually develop as a result of changes in loading or frequency, or by oxidation of the fracture surface during periods of crack arrest from intermittent service of the part. Thus, the beach marks and thumbnail patterns observed on the fracture surface indicated that a primary fatigue crack initiated within the circled area identified in Figures 2a and 2b and the secondary fatigue cracked initiated within a similar region on the side of the stem opposite the primary fatigue crack. However, the specific crack origins could not be identified by visual and stereomicroscopic examinations.

The two fatigue cracks propagated in opposite directions. The primary fatigue crack propagated much farther across the diameter of the stem, as indicated by the location of the beach mark identified by the small arrow in Figure 2a, than did the secondary fatigue crack. The final fracture zone between the two opposing fatigue cracks was not identified. The zone was apparently very small, since the tips of the two cracks apparently were very close to each other when final fracture of the remaining section occurred.

The presence of two opposing fatigue cracks indicated that the cracks initiated from reverse-bending stresses. The magnitude of those stresses were indicated by the very small final-fracture zone to be nominally very low. Either the primary crack initiated and propagated under somewhat higher bending stresses than did the secondary crack, or the primary crack initiated earlier and propagated for a longer time than did the secondary crack.

A visual examination of the plug revealed six areas of wear about 1 1/4-inch square on the cylindrical surface of the lower plug. The wear areas were spaced at 60-degree intervals around the plug. The worn surfaces had the appearance of a highly-polished, peened or hammered

surface. Relative to the fracture surface features, two opposing wear areas were in alignment with the origin regions of the two opposing fatigue-cracks.

Measurements of the depths of wear on the lower plug were made using a dial-displacement gage while the plug was rotated 360 degrees in a lathe. The gage was adjusted to zero at a location on the cylindrical surface midway between two wear areas. The results of the depth measurements are recorded in Figure 3. Two adjacent wear areas were worn to depths of 0.020 and 0.024 inch, respectively. The depths of the remaining wear areas were 0.006 inch or less. The primary fatigue-crack-origin region was found to be aligned with, and on the same side of the valve stem, as was the area, Wear-Location 1 in Figure 3, that was worn to a depth of 0.020 inch. The secondary fatigue-crack origin was on the same side and aligned with the wear area identified in Figure 3 as Wear-Location 2.

Scanning-Electron-Microscopic Examinations. The surface of the stem-half of the fracture was examined in the scanning electron microscope (SEM) in the as-received condition and after removal of corrosion products by electrochemical cleaning techniques. The SEM examinations were concentrated in the region of the origin of the primary fatigue crack. A SEM micrograph of the origin region before cleaning is shown in Figure 4.

The origin region exhibited considerable mechanical damage, which is evident as smooth, dark-gray areas in Figure 4a. Figure 4a also shows, in the region of letter T, the portion of the thumbnail pattern nearest to the origin of the fatigue crack. Fracture ridges within the thumbnail appeared to radiate outward from the approximate location in Figure 4a of the letter X, which was subsurface and within the fillet weld. The point or site from which fracture ridges diverge usually is the location of the crack origin. No evidence of a crack origin was observed in the immediate region identified by the letter X. The region exhibited much mechanical damage which may have obliterated evidence of an origin.

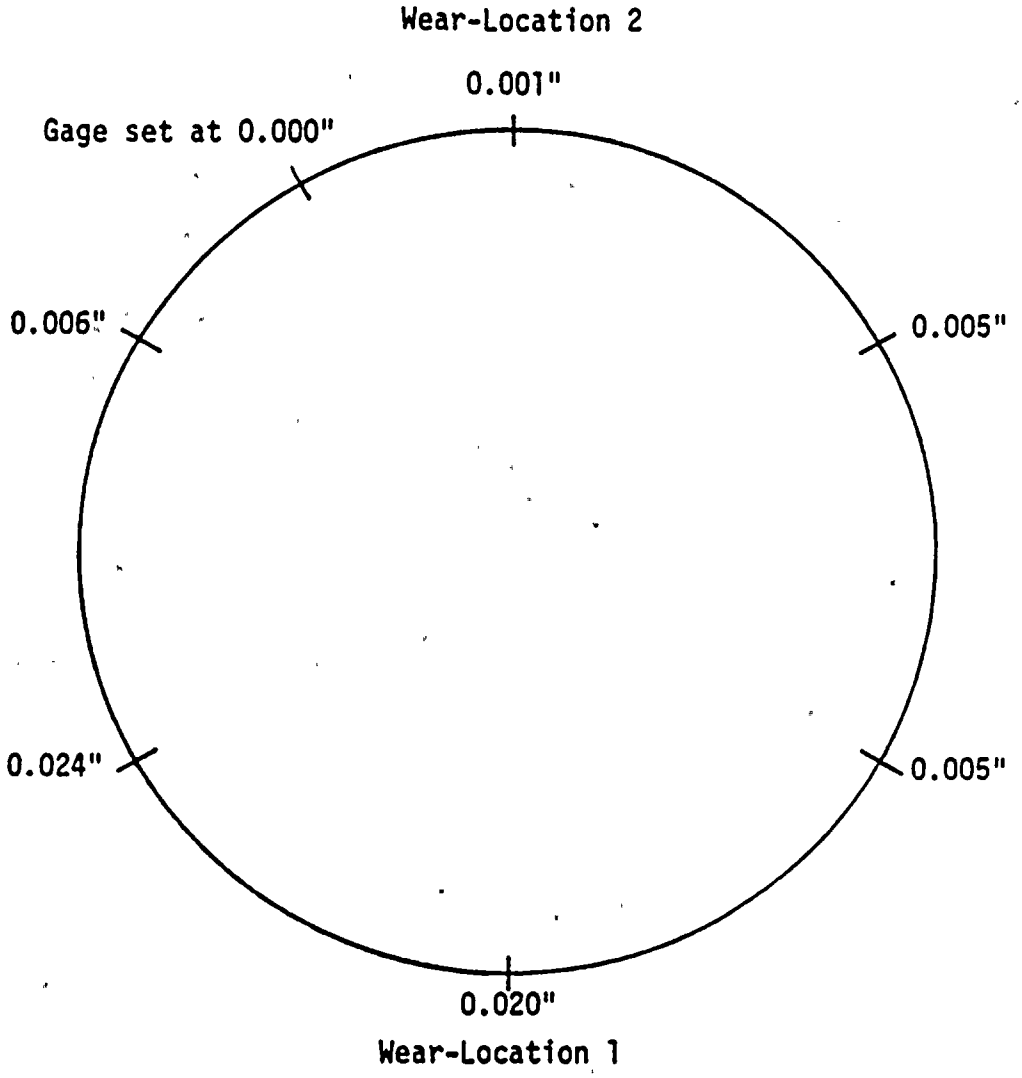

FIGURE 3. SKETCH SHOWING THE DEPTH OF WEAR AT THE 60-DEGREE WEAR LOCATIONS ON THE LOWER PLUG

The primary fatigue-crack origin was approximately in alignment with, and on the same side of the stem, as was the side of the lower plug at Wear-Location 1 in the sketch. Similarly, the secondary fatigue-crack origin was in alignment with Wear-Location 2 in the sketch.

a. Origin Region of the Primary Fatigue Crack

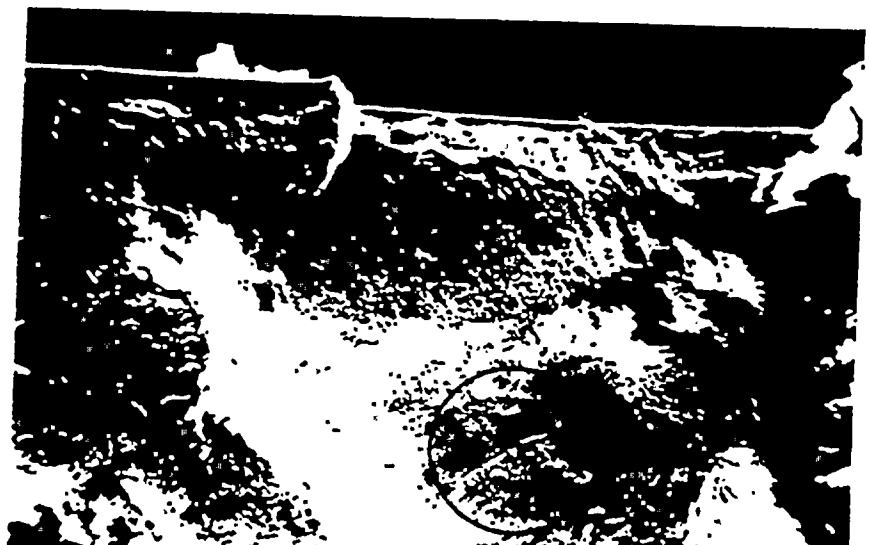

b. Circled Area in (a) Above at a Higher Magnification

FIGURE 4. FRACTURE FEATURES OBSERVED IN THE CRACK-ORIGIN REGION BY SCANNING ELECTRON MICROSCOPY BEFORE CLEANING

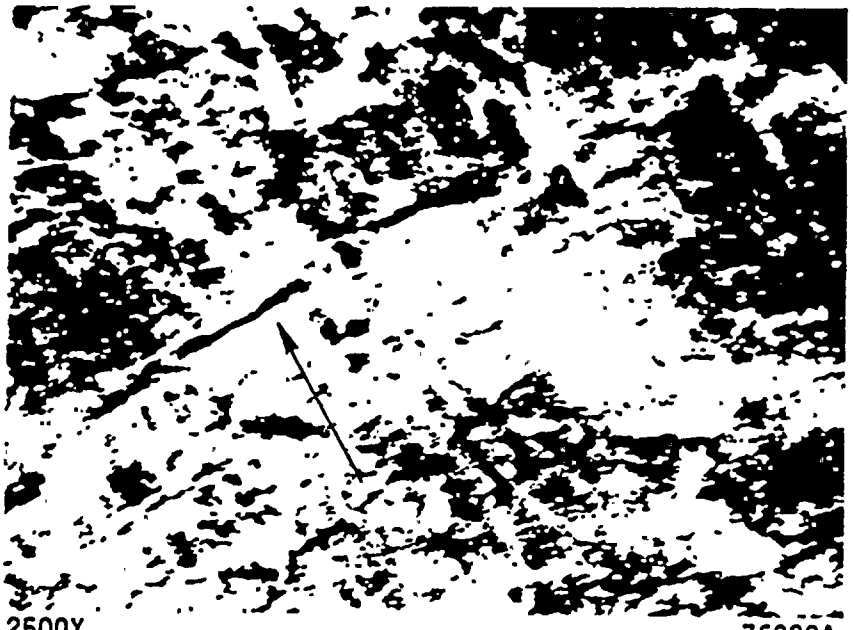

c. Apparent Fatigue Striations Observed at a Higher Magnification Within the Encircled Area in Figure 4b
(The arrow indicates the direction of crack propagation.)

FIGURE 4. CONTINUED

Figure 4b shows the fracture surface in weld metal within the circled area in Figure 4a. The circled area in Figure 4b is shown at a higher magnification in Figure 4c. Striations, which appear to be fatigue striations, are evident in Figure 4c. The curvature of the striations indicated that the direction of crack propagation was in the direction of the arrow in Figure 4c, which was outward to the surface of the fillet weld; that direction of crack propagation also suggested that the crack origin was subsurface and in the general vicinity of Location X in Figure 4a.

An area of corrosion products observed on the fracture surface within the primary thumbnail pattern is shown in Figure 5. Those corrosion products were characterized by a cracked appearance and the presence of chlorine that was detected by EDS microprobe analysis. Very few areas were observed that exhibited this type of corrosion products. Other corroded areas did not exhibit the cracked appearance nor was the presence of chlorine detected in those areas.

The cleaned surface of the fracture in the primary origin region is shown in Figure 6. Figure 6a is the same area as that in Figure 4a and shows essentially the same macroscopic features. No specific crack initiation site was identified within the suspected origin region. However, fatigue striations, other than those shown in Figure 4c, were observed. Those striations are shown in Figures 6c and 6d, which are higher magnification fractographs of the encircled region identified in Figure 6b. The curvature of the striations, like those shown in Figure 4c, indicated that crack propagation proceeded outward to the surface of the fillet weld from an initiation site that was subsurface and apparently within weld metal.

Typical features observed on the surface of the fracture across the valve stem are shown in Figure 7. Those features included very fine fatigue striations; examples are evident between pairs of arrow heads shown in Figure 7b.

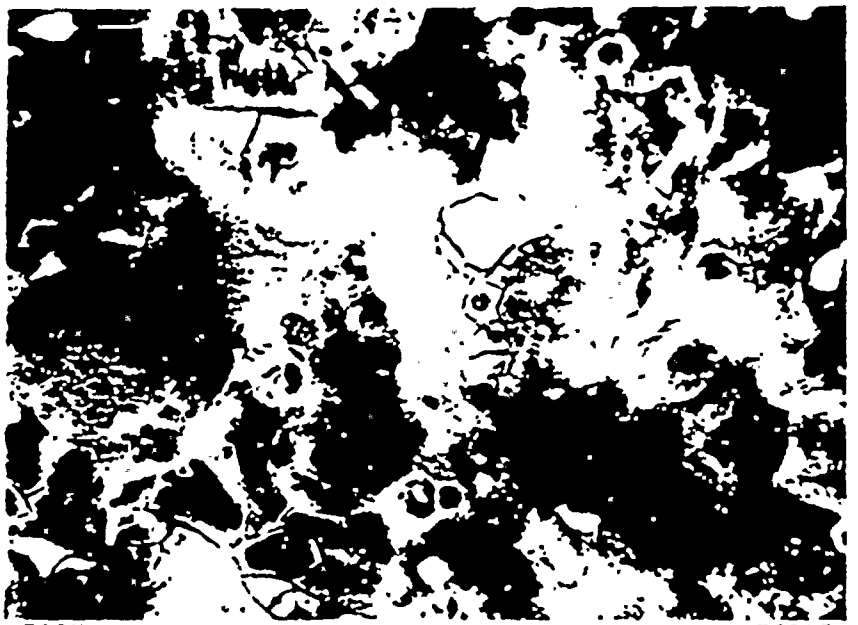

FIGURE 5. CORROSION PRODUCTS WHICH CONTAINED CHLORINE ON THE FRACTURE SURFACE

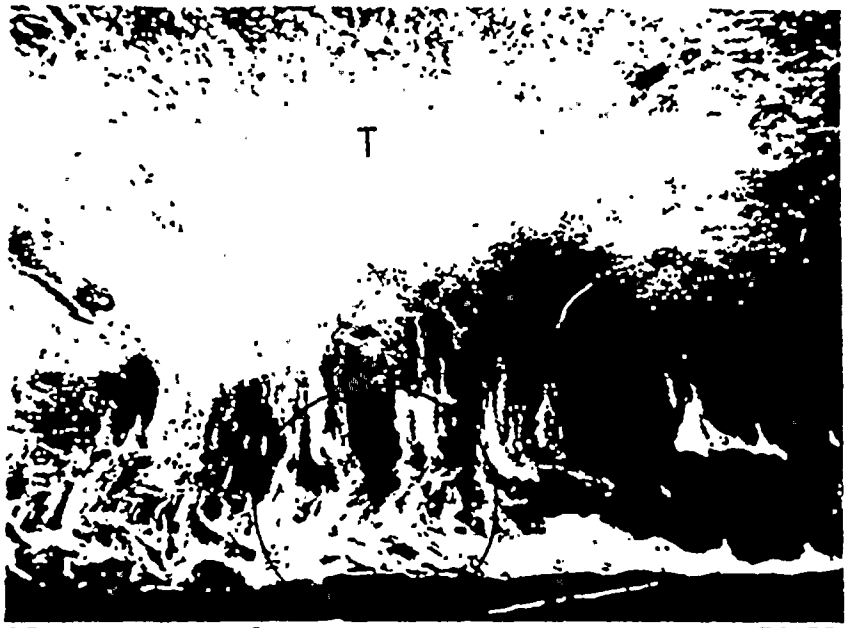

15X 76055

a. Origin Region of the Primary Fatigue Crack (Same area as that shown in Figure 4a.)

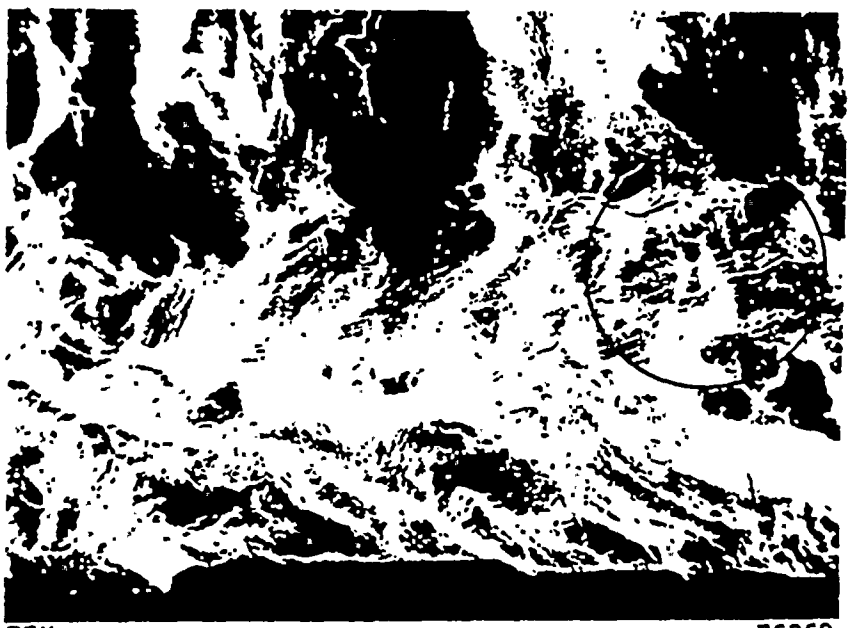

75X 76060

b. Circled Area in (a) Above at a Higher Magnification

FIGURE 6. FRACTURE FEATURES OBSERVED IN THE CRACK-ORIGIN REGION BY SCANNING ELECTRON MICROSCOPY AFTER CLEANING

c. Circled Area in (b) at a Higher Magnification Showing Apparent Fatigue Striations

(The arrow indicates the direction of crack propagation.)

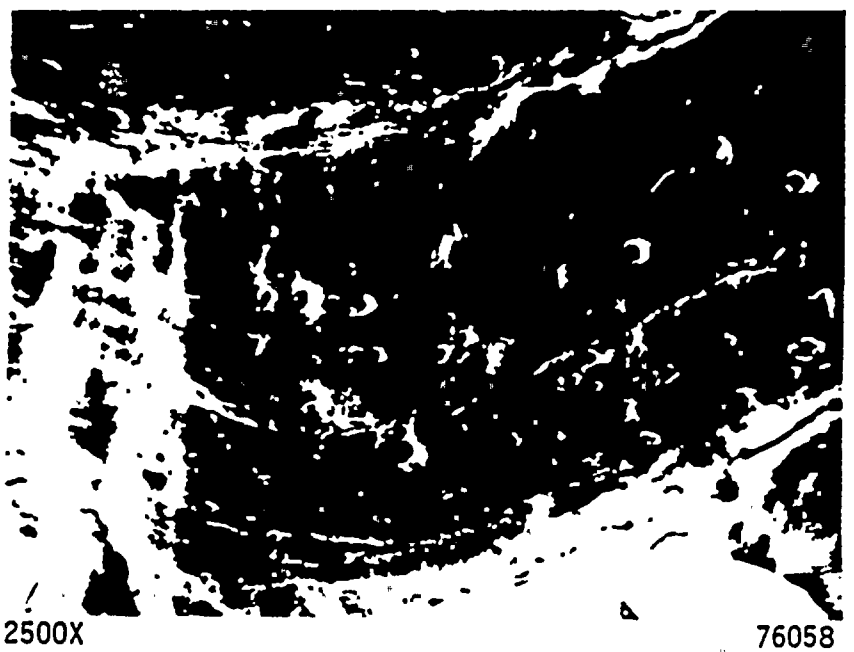

d. Higher Magnification of Apparent Fatigue Striations Shown in (c) Above

FIGURE 6. CONTINUED

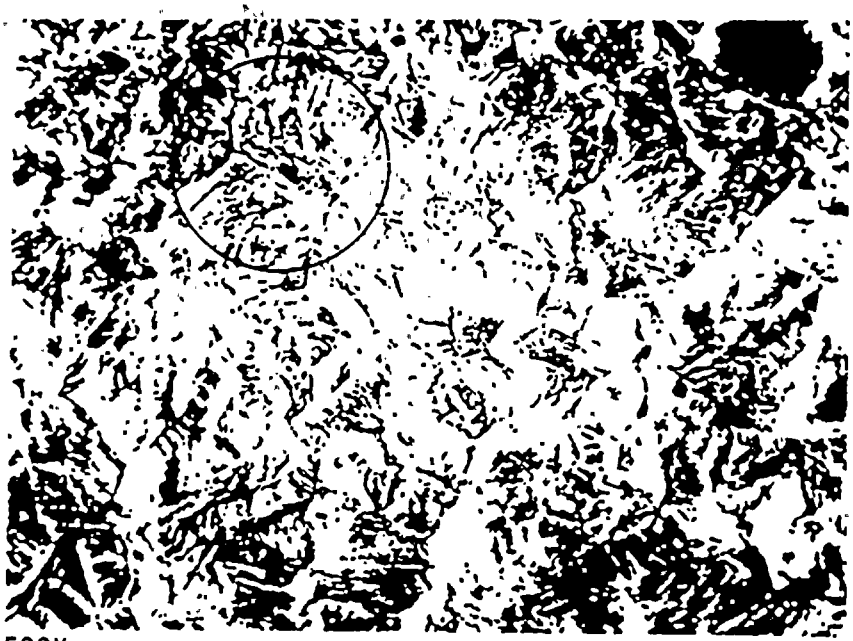

500X 76061

a. An Area Within the Thumbnail Pattern in the General Region of Letter T in Figure 6a

2000X 76062

b. Very Fine Fatigue Striations (between pairs of arrowheads) Within the Area Encircled in (a) Above

FIGURE 7. TYPICAL FEATURES OBSERVED ON THE FRACTURE SURFACE IN THE VALVE STEM

Metallographic Examinations

A cross section of the matched fracture halves was prepared metallographically for examination. The cross section intersected the general region of the crack origin that was indicated by the primary thumbnail pattern on the fracture surface. The metallographic specimen was ground, polished, etched and examined successively seven times at increments of 5 to 10 mils, in an attempt to intersect and identify a surface or subsurface flaw, or other microstructural abnormality from which the primary fatigue crack initiated. No crack initiator was identified during the examinations of those seven serial sections.

The fracture was observed in the metallographic sections to be transgranular through the weld metal and across the stem. The microstructure of the weld metal was typical of the microstructure of Type 316 stainless steel weld metal in the as-welded condition. The microstructure of the stem was typical of the microstructure of wrought and annealed Type 316 stainless steel. No evidence of sensitization in the microstructure of the weld-heat-affected zone of the stem was observed. A photomacrograph of one of the seven serial sections is shown in Figure 8a. The primary fatigue crack was located on the side of the stem identified by the arrow in Figure 8a; a portion of the fillet weld and crack is shown in Figure 8b at a higher magnification.

Discussion

The results of the fractographic examinations indicated that the mode of crack propagation was primarily fatigue. The mode of crack initiation, although not observed on the fracture surface since a specific site of crack initiation was not identified, apparently was fatigue also. The macroscopic features of the primary fatigue-thumbnail pattern and the microscopic fatigue striations, which were observed, indicated that the general vicinity of the initiation site was subsurface near the root of the weld. The nature of a crack initiator at that location would most likely be that of a weld flaw, such as a hot crack or weld-metal pore. Flaws of that nature are frequently stress-raisers

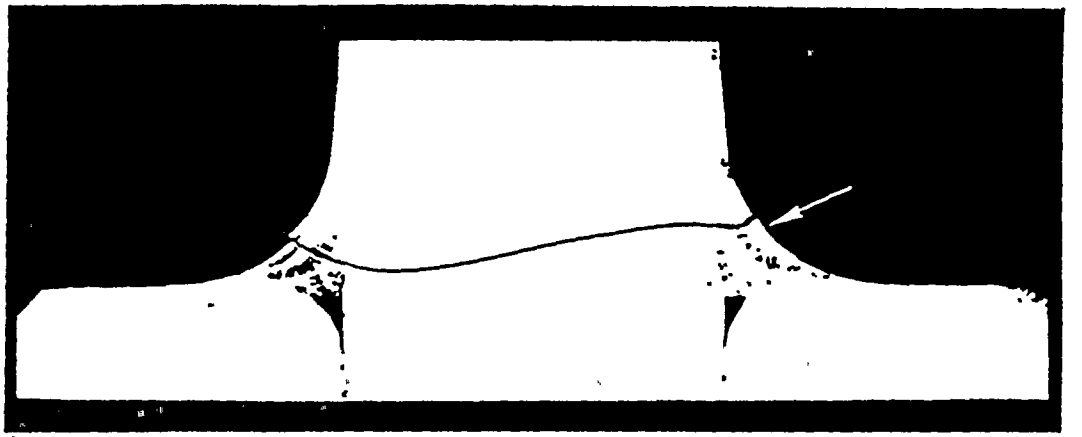

2X 2N725

a. Cross Section of Matched Fracture Halves Through the Primary Origin Region at the Fillet Weld Indicated by the Arrow

25X 2N726

b. Higher Magnification of the Fillet Weld Indicated by the Arrow in (a) Above

FIGURE 8. A METALLOGRAPHIC CROSS SECTION THROUGH THE PRIMARY FATIGUE-CRACK-ORIGIN REGION

about which the magnitude of the resultant stress concentration can exceed the fatigue strength of the metal. Hence, a fatigue crack initiates in the adjacent metal and propagates.

The stresses involved in the initiation and propagation of the fatigue failure were indicated to be reverse-bending stresses. The presence of residual stresses induced by welding would be additive to the service stresses. The bending stresses apparently developed during wear at the lower plug. As the wear, particularly on one side of the lower plug, progressed to greater depths, the clearance between the body of the valve and the lower plug increased, and the welded joint between the plug and stem was subjected to a bending moment. The bending stresses would be expected to increase as the depth of wear on the lower plug increased. Ultimately, the magnitude of those stresses plus residual-welding stresses, multiplied by a stress-concentration factor of an internal flaw, if present, apparently was sufficient to start a fatigue crack.

Conclusions

The results of the metallurgical investigation of the plug and valve stem failure led to the following conclusions:

(1) The mode of crack propagation was fatigue.

(2) A specific crack origin was not identified, but the location of the origin appeared to be subsurface within the fillet weld metal.

(3) Fatigue crack propagation was induced principally by reverse bending stresses.

(4) Bending stresses apparently developed as a result of wear on the lower plug. The bending stresses probably increased as the depth of wear increased.

(5) The microstructures of the weld metal and stem were normal.

(6) The chemical compositions of the weld metal and stem were within the composition limits of Type 316 stainless steel. The chemical composition of the plug was apparently that of a cast stainless steel alloy, CF8M.

Recommendations

The results of the investigation indicated that, to prevent a failure of this type in the plug and valve stem, the stress concentration in the fillet weld and the bending stresses should be minimized. Two recommendations are suggested to accomplish this.

(1) Increase the diameter of the stem at the welded joint and use a streamline, elliptical or parabolic form of fillet instead of a constant radius (circular fillet).

(2) Consider a change of design and/or material for the plug to reduce the amount of wear that occurs on the lower end of the plug.

PART TWO: STAINLESS STEEL WELD METAL FROM FEEDWATER PIPE

Introduction

The failure of the stainless steel welded pipe occurred in a circumferential weld between a carbon steel pipe and a 5 percent chromium steel pipe, which were reported to be about 8 to 10 inches in diameter. The welded pipe was from the suction side of the feedwater pump and contained feedwater at 316 F and an internal pressure of about 170 psig. The pipe was reported to have been considerably repair welded at least 18 years ago. The repair welding process was not reported to Battelle. The failure was a crack in the weld metal which eventually propagated through the joint and allowed feedwater to leak into insulation on the outside of the pipe. The type of insulation was not reported to Battelle. A boat sample containing a portion of the crack was furnished to Battelle for a metallurgical investigation of the cause of the crack.

Summary

A crack contained in a weld-metal boat sample removed from a circumferential austenitic stainless steel weld was investigated to determine the most probable cause of the failure. The investigation involved primarily a chemical analysis of the weld metal, fractographic studies of the crack surface, and metallographic studies of a cross section of the crack.

The results of the investigation indicated that the crack most likely was caused by intergranular stress-corrosion cracking (IGSSC). The weld metal was found to be sensitized and, thereby, was susceptible to IGSSC. The stresses which assisted intergranular corrosion were believed to be a combination of residual welding stresses and applied service stresses.

A recommendation was made to eliminate sensitization by using a stabilized austenitic welding electrode, such as E347, and by avoiding

prolonged heating or slow cooling of the weld metal in the temperature range of 1000-1500 F.

Results of Laboratory Examinations

Chemical Analysis

A chemical analysis of the weld metal from the boat sample was obtained using emission spectrographic analytical techniques. The results of the chemical analysis are presented in Table 3. Included in Table 3 are the composition limits for an austenitic stainless steel electrode, EX310T-X, which is used for flux cored arc welding (FCAW). An austenitic stainless steel electrode, E310, which is used for shielded metal are welding (SMAW) has composition limits similar to those of EX 310T-X. The results of the chemical analysis of the weld metal from the boat sample indicated that the welding electrode used for repair welding was most likely the Type 310 stainless steel electrode used for either FCAW or SMAW.

Fractographic Examinations

The boat sample containing the crack was sectioned lengthwise in half. The portion of the crack in one half of the boat sample was broken open in the laboratory to expose the fracture surface for fractographic examinations. Those examinations were made in the scanning electron microscope (SEM). The cut face of the other half of the boat sample, which contained the remainder of the crack, was mounted and prepared metallographically for examination.

SEM examinations of the fracture surface were performed before and after cleaning the surface since corrosion products and discolorations were evident. The evidence of corrosion and discolorations was most prominent on the surface of the fracture nearest the inside surface of the welded pipe and the evidence diminished across the fracture surface toward the outside surface.

TABLE 3. EMISSION SPECTROGRAPHIC ANALYSIS OF THE CHEMICAL COMPOSITION OF THE WELD METAL FROM THE BOAT SAMPLE

Element	Content, weight percent	
	Boat Sample, weld metal	FCAW Electrode, EX310T-X[(a)]
Carbon	0.12	0.20
Manganese	1.61	1.0-2.5
Phosphorus	0.022	0.03
Sulfur	0.010	0.03
Silicon	0.50	1.0
Copper	0.008	0.5
Tin	0.012	
Nickel	19.7	20-22.5
Chromium	26.5	25-28
Molybdenum	0.06	0.5
Aluminum	0.005	
Vanadium	0.05	
Niobium	0.01	
Zirconium	0.002	
Titanium	0.015	
Boron	0.0002	
Calcium	0.0032	
Cobalt	0.08	
Tungsten	0.00	

(a) Composition limits for a Type 310 stainless steel electrode used for flux cored arc welding (FCAW). ASM Metals Handbook, Vol. 6, Ninth Edition.

A low-magnification SEM micrograph of the fracture surface before cleaning is shown in Figure 9. Crack propagation appeared to be along columnar, weld-metal grain boundaries which gave a "woody" appearance to the fracture surface. EDS microprobe analyses of several areas on the uncleaned fracture surface did not detect the presence of any unusual elements, such as chlorine or sulfur that might indicate a specific ionic specie was responsible for the corrosion attacks.

A typical area of the fracture surface after cleaning is shown in Figure 10. Most of the fracture surface was relatively smooth, which is typical of an intergranular mode of crack propagation along columnar grains of the weld metal. However, small particles, some of which are indicated by arrows in Figure 10, were observed in the smooth intergranular surfaces of the fracture. Those particles indicated the presence of an intergranular phase.

Metallographic Examinations

The portion of the metallographic cross section of the boat sample which contained the crack through weld metal is shown in Figure 11a. Intergranular fracture along the columnar grain boundaries of the weld metal is evident in Figure 11a. Figure 11b shows a portion of the intergranular fracture at the outside surface of the weld in a plane different from that shown in Figure 11a. In addition to the intergranular fracture, Figure 11b shows two small transgranular cracks in the outside surface of the weld; those cracks are identified in Figure 11b by arrows. Four other small transgranular cracks were observed elsewhere in the outside surface of the weld. One of the other four cracks is shown in Figure 12. All of the small transgranular cracks exhibited crack-branching; the appearance of the cracks was typical of transgranular stress-corrosion cracking in stainless steel. However, none of the cracks appeared to be associated with, or related to, the intergranular fracture through the weld metal.

The microstructure of the weld metal, revealed by etching the specimen with a solution consisting of 97 ml. conc. HCl, 3 ml. conc. HNO_3, and 1/2 g $CuCl_2$, exhibited the presence of an intergranular phase.

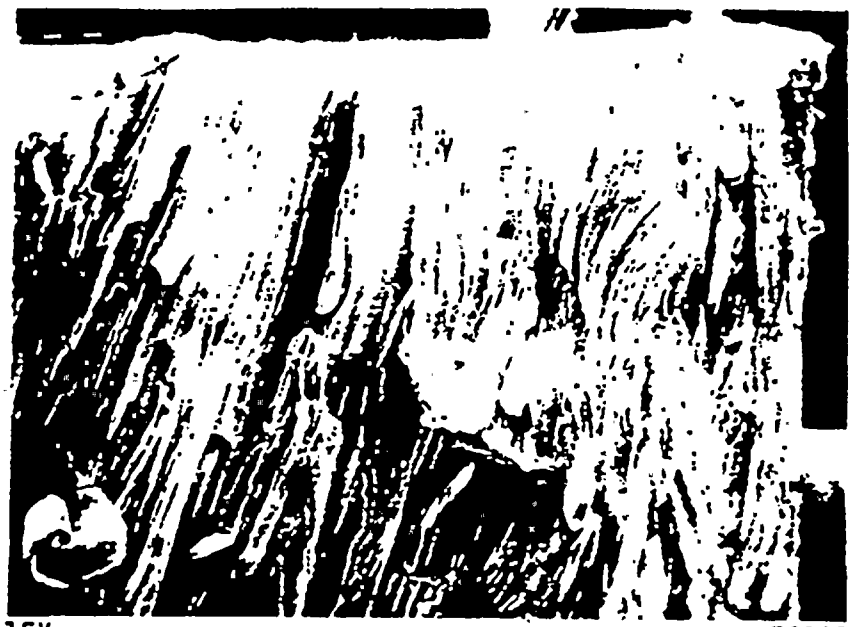

15X 76042

FIGURE 9. "WOODY" APPEARANCE OF THE SURFACE OF THE WELD-METAL CRACK IN THE BOAT SAMPLE

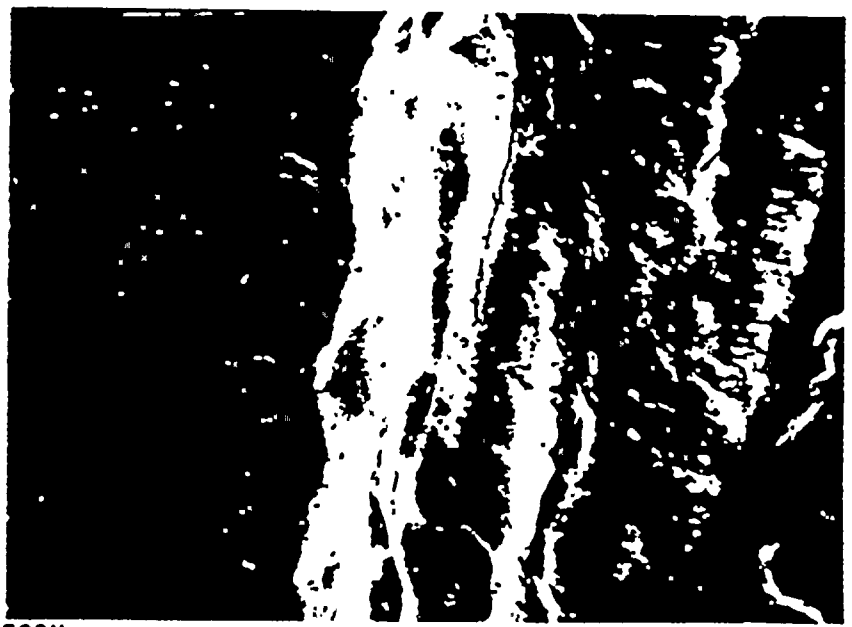

500X 76070

FIGURE 10. TYPICAL AREA OF THE CRACK SURFACE AFTER CLEANING

Arrows identify some of the intergranular particles.

10X 2N727

a. Section Completely Across the Weld (Boat Sample)

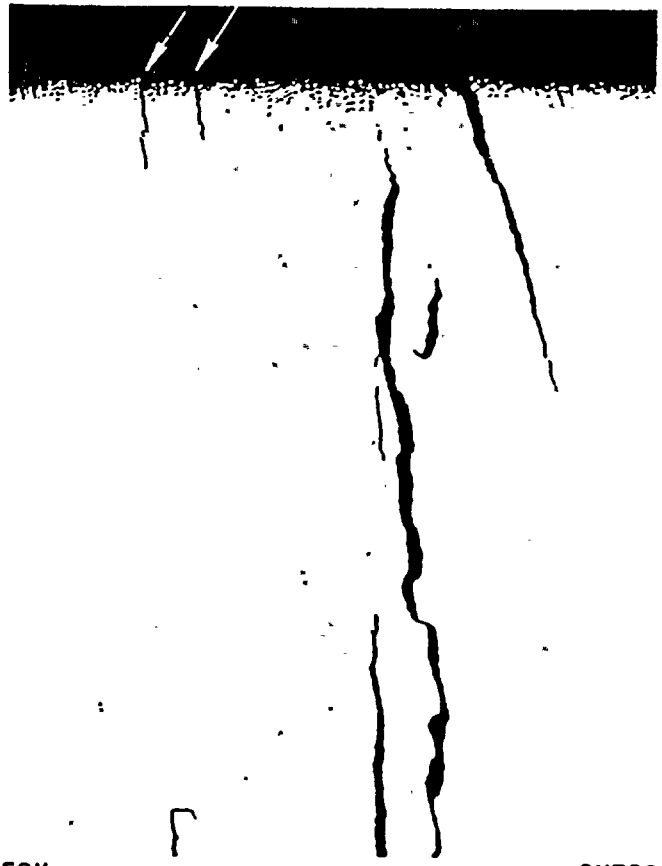

50X 2N728

b. Cross Section of the Weld at the Outside Surface (arrows identify secondary transgranular cracks)

FIGURE 11. METALLOGRAPHIC CROSS SECTION OF THE BOAT SAMPLE SHOWING THE NATURE OF THE INTERGRANULAR FRACTURE THROUGH WELD METAL

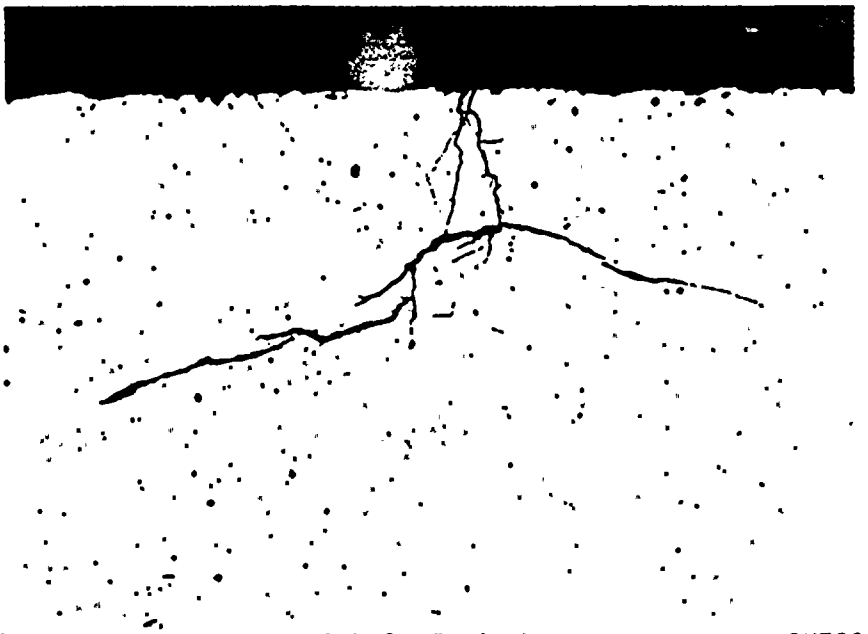

250X Lightly Etched 2N729

FIGURE 12. ONE OF THE SMALL TRANSGRANULAR STRESS-CORROSION CRACKS OBSERVED IN THE OUTSIDE SURFACE OF THE WELD METAL

Figures 13a and 13b show examples of the intergranular phase in two areas of the weld metal where the phase was displayed most prominently. The phase was evident in virtually all of the weld-metal grain boundaries observed in the metallographic specimen. Occasionally, the phase exhibited a lamellar morphology, as shown in Figure 13b.

The circled area shown in Figure 13b was selected for the wavelength-dispersive (WDS) analysis. WDS is capable of detecting the presence of elements of atomic Number 5, boron, and higher. The intergranular phase was identified as a carbide by X-ray WDS microprobe analysis in conjunction with the scanning electron microscope. A SEM micrograph (secondary-electron image) of the area is shown in Figure 13c at a higher magnification. An X-ray distribution map of carbon in the area is shown in Figure 13d. The X-ray distribution map reveals a concentration (high-density of white dots in the X-ray distribution map) of carbon in the intergranular phase. A slight concentration of chromium and depletion of iron relative to the concentration of those elements in the surrounding weld-metal matrix also were detected in the phase by the WDS X-ray counts for those elements. Thus, the intergranular phase was most likely an iron-chromium carbide.

Discussion

The most significant results of the laboratory examinations were (1) the presence of discolorations and corrosion on the fracture surface which was more evident toward the inside surface than toward the outside surface of the pipe, (2) a fracture mode identified as intergranular, and (3) the presence of an intergranular carbide phase. The distribution over the fracture surface of corrosion and discolorations indicated that the failure most likely started on the inside surface of the circumferential pipe weld. The surface of the earlier stages of crack propagation were apparently exposed to the corrosive environment for longer periods of time. The presence of intergranular carbides in the weld metal constituted a sensitized condition of the weld metal. Stainless steels derive their resistance to corrosion principally from the presence of chromium. The formation of intergranular iron-chromium

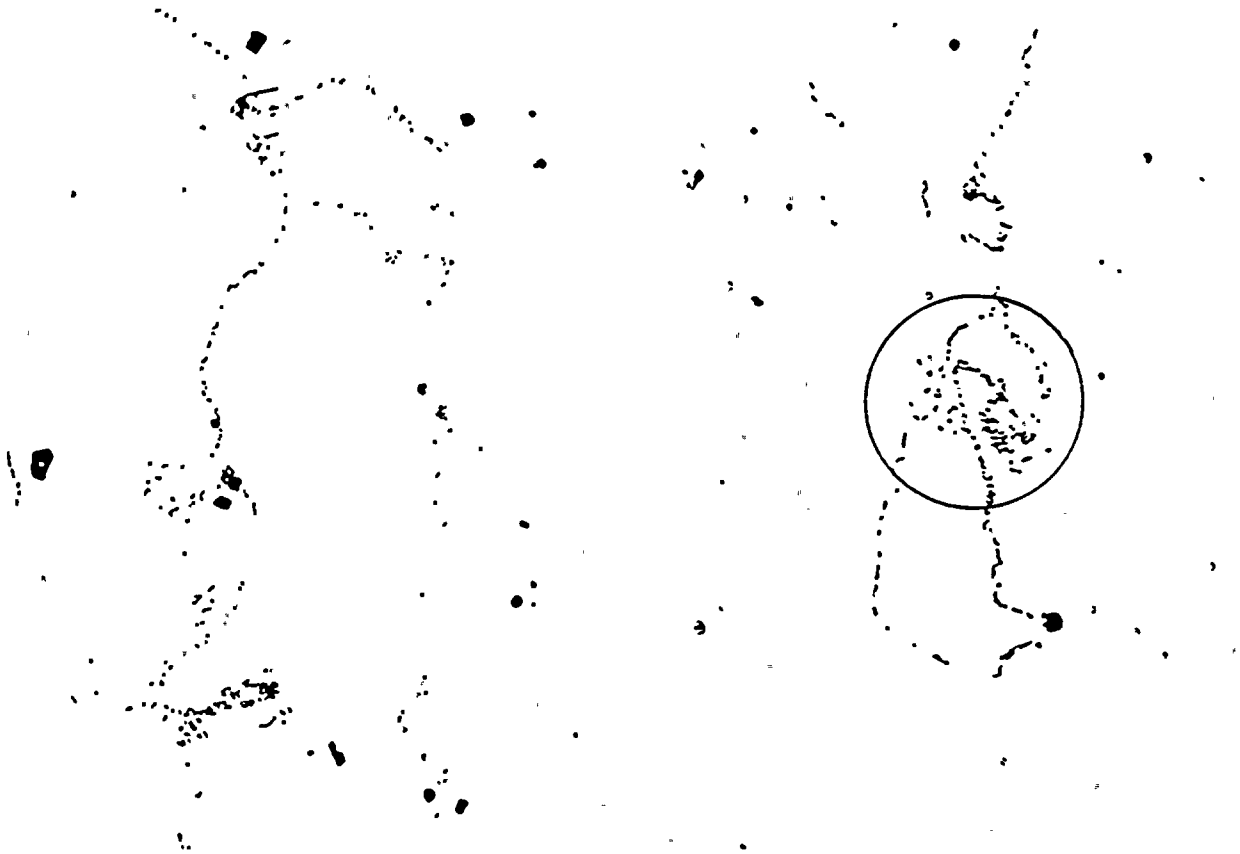

1000X Etched 2N731 (a)

1000X Etched 2N730 (b)

FIGURE 13. EXAMPLES OF THE INTERGRANULAR CARBIDE PHASE OBSERVED IN THE WELD-METAL GRAIN BOUNDARIES

3600X Etched P989

c. Secondary Electron Image of the Area Encircled in (b) at a Higher Magnification

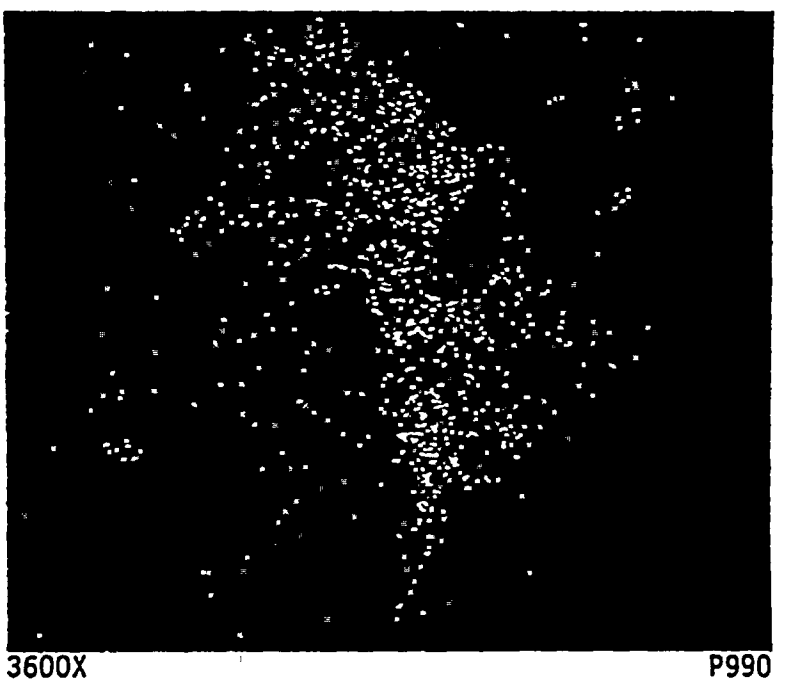

3600X P990

d. X-ray Distribution Map of Carbon in the Area Shown in (c) Above

FIGURE 13. CONTINUED

and/or chromium carbides (sensitization) depletes the areas adjacent to the grain boundaries of chromium and those areas become susceptible to intergranular corrosion attack. Stainless steels stabilized with additions of niobium (columbium) or titanium, which combine with carbon and prevent chromium carbide precipitation, do not normally become sensitized. The composition of the weld metal indicated that unstabilized stainless steel welding electrodes were used for the repair weld.

Unstabilized stainless steel becomes sensitized if heated to temperatures in the range 1000 to 1550 F, or if cooled slowly through that temperature range. High heat input and low travel speeds induce sensitization in stainless steel weld metal. Welding processes that have a high potential for carburizing stainless steel, such as dry fuel-gas welding, which also has a high heat input, increases the sensitization of weld metal.

Intergranular corrosion of sensitized material may occur with or without stress. The former failure mode is often referred to as intergranular stress-corrosion cracking (IGSCC). IGSCC occurs most often in corrosive environments of polythionic acid solution or of high-temperature oxygenated water. The specific corrosive element which apparently led to the intergranular attack of the stainless steel weld metal, was not identified by the laboratory examination performed. However, oxygenated feedwaters are known to cause ISCC. Although the welded pipe was reported to be under a relative low stress, residual stresses in weldments are often sufficient to sustain either SCC or IGSCC. Conventional transgranular SCC, such as the secondary SCC observed on the outside surface of the weld metal, usually occurs in chloride or caustic solutions. The observed transgranular SCC probably occurred after leakage of the pipe. The moisture on the outside surface of the weld metal may have leached chlorine from the insulation which, combined with residual and/or applied stresses, led to the observed transgranular SCC.

Conclusions

The results of the metallurgical investigation led to the following conclusions:

(1) The failure of the weld metal was most likely caused by intergranular stress-corrosion cracking (IGSCC).
(2) The weld metal was sensitized and thereby was susceptible to IGSCC.
(3) The corrosive environment was not identified. The environment might have been high-temperature oxygenated feedwater.

Recommendations

In order to eliminate sensitization and the subsequent potential IGSCC in austenitic stainless steel weld metal, it is recommended that a stabilized stainless steel welding electrode, such as E347, be used, and that prolonged heating or slow cooling of the weld metal through the temperature range of 1000 to 1550 F be avoided.

APPENDIX F

NIAGARA MOHAWK

SURVEILLANCE REPORT

FACILITY: _____ PAGE 1 OF _____

QA SECTION/GROUP: Materials Quality Engineering REPORT NO. SR8855001

RESPONSIBLE ORGANIZATION: Nuclear Engineering DATE: Dec. 29 [redacted] 98 Jan. 11 [redacted] 98

SUBJECT: Feedwater Pump #13, Impeller (Turbine driven)

CHECKLIST NO., REV. & TITLE OR GOVERNING DOCUMENTS _____

SCHEDULED: YES ☐ NO ☒ NUCLEAR SAFETY RELATED: YES ☐ NO ☒ 10CFR50 APP. B CRITERIA: N/A

PERSONNEL CONTACTED: M. J. Falise, R. A. Cushman, D. L. Pracht, K. Dahlberg, Art Smith, Bob Christensen, F. Hawksley of NMPC and Bob Loveless of Worthington

On Tuesday afternoon, December 29, and again on Monday January 11, I visually inspected the impeller for Feedwater Pump #13. This is the turb driven pump, built by Worthington. The impeller is a one piece casting of CA6NM alloy, provided to us by Worthington Group of McGraw Edison Co., Buffalo, New York on PO#22054 of 7/15/84. This impeller has been in-service since the completion of the 1986 Nine Mile One refueling outage.

Background

In its present condition, the impeller has a piece missing from the leading edge of one vane, about 1 7/8" along the edge and extending about 1⅛" into the vane. This is enough to cause severe vibration of the impeller at its operating speed of 5020 RPM. Each of the six vanes has extensive cavitation errosion on the suction side (as opposed to the pressure side). Each vane has a different pattern but in general the cavitation damage begins within ½" of the leading edge, is at its worst at 1 to 2 inches from the leading edge, and continues for various distances up the suction side of the vanes. The severity

continued.....

ACCEPTABLE: YES ☐ NO ☐

OPEN ITEMS:

CAR(S)/NCR(S) INITIATED:		TREND CODES:	
Roger H Todd	Jan 15, 1988	Robert O. Norris	1-15-88
PREPARED BY:	DATE	APPROVED BY:	DATE

of cavitation damage has dictated that the rotor be replaced at each refueling outage. The material selected, CA6NM alloy, has high hardness (R 23 minimum) combined with high toughness and is generally considered a good choice for high resistance to cavitation damage.

Observations

Observations on the impeller are as follows. One vane of the six-vaned impeller was missing a section at the intake edge of the vane, as stated before. In Figure 1, this is indicated as vane A. A second vane, B in Fig. 1, upstream of vane A, carries a dent (1/4" wide) on the suction side of the leading edge. The centerline of the leading edge is slightly displaced by the dent. The third vane, at C in Fig. 1, has an unusually bright spot on the leading edge where the vane joins the outer rim of the intake circle. This spot is free of oxide and crud. No surface effects of impact can be seen.

A sketch of the missing portion of a vane is shown in Figure 2. The broken surface extends from A to B to C. At A the surface is hackley, rough, seemingly porous - like the broken surface of a tensile specimen. This rough surface has about equal dimensions, that is length and width are about the same as the thickness of the vane at that point. As sketched in Figure 3A, there is what appears to be a beach mark separating the hackley zone at A from an adjacent very smooth area. The midportion between A and B displayed faint cherron marks when observed on December 29. Only a very slight suggestion of those chevron marks were found on Jan. 11. The broken surfaces appear to have been rubbed with rags, and scratches from tools exist between A and B.

The corner at B is very smooth and bright indicating considerable scrubbing action had occurred between the broken parts, as in fatigue. The region from B to C displayed about half the thickness rubbed smooth; also, a sizeable portion of the thickness was missing because of cavitation erosion on the low pressure side of the vane. A beach mark near C outlined an area of hackley fracture which terminated in a hinge lip as sketched in Figure 3B.

The impeller surface was covered overall with a brown layer of iron oxide/crud. Survey Tags stated contamination levels were 150 dpm/100 sq. cm. No attempt was made to scrub or clean any surfaces being examined since necessary facilities were not available.

Discussions

The crack which caused the separation of a portion of one vane, originated within the vane, not at the edge. The crack propagated almost entirely around the roughly circular triangle until only two small supports remained. These were at points A and C in Fig. 2. This condition prevailed for a considerable period of time, allowing beach marks to develop near A and C; and buffed surfaces at the points observed. An event occurred which overloaded the remaining supports, causing rupture of the remaining support metal at A. At that moment the vane was still pushing water into the

intake of the impeller. Reaction forces caused the triangular piece to bend at C and move upstream in relation to the water flow direction. The hinge at C is perpendicular to a line drawn from A to C. The bending action broke the attachment at C and the piece was then free to follow the water flow through the pump and into the piping system. Material of this alloy cannot be easily broken up; therefore it is probable this piece (1 7/8 x 1 1/4 inches in roughly triangular shape) passed through the piping until stopped at the upstream tube sheet of the fifth-stage preheater. The tubes of the preheater are 1/2" diameter.

The cause of this cracking would have been a casting defect, such as a hot tear, cold shut, shrinkage or a combination of these. Similar defects have been found in cast runners of this same alloy, obtained for hydrostation use during the past five years. The casting defect would have been made more critical by cavitation erosion.

Conclusion

It is my opinion that the primary cause of failure was a casting defect in the affected vane which was activated by removal of surface material by cavitation erosion. The final event leading to failure was simply a larger-than-normal pressure surge or pulse within the system. If the casting defect had not been present, this impeller would have reached its replacement service life without difficulty.

Recommendations

Future replacement impellers should have requirements for inspection to preclude acceptance of any impeller containing hot cracks, excessive shrinkage voids, cold shuts or excessive porosity. The replacement impeller now being installed should be inspected during the 1988 refueling outage. Where geometry permits, wet fluorescent magnetic particle technique should be used. Where that technique cannot be used, the dye penetrant technique can be substituted. Good visual examination after surface cleaning should be the initial NDE technique in any case. Other NDE techniques would be necessary only if the visual and mag particle (or dye pen.) examinations turn up areas of questionable quality.

If any additional information is needed from the existing damaged impeller, the work involved should follow these guidelines:

1. Facility must be licensed to handle radioactive contamination.
2. Impeller must be cleaned in steps to remove surface scale, crud and oxides, so as to expose clean metal for examination without disturbing any physical features present on the metal surface. No chemical attack of the metal can be permitted.
3. Examine under magnification and selected special illumination.

4. Photograph as information is developed at required magnification.
5. Be prepared to cut cross-sections and perform metallography at points of special interest identified in preceding steps.

Purposes of supplementary examination would be:

A. To identify the nature and origin of the defect(s) causing the crack.
B. To determine if the offending defect occurred at several points within the impeller or if it was a unique occurrence.
C. To recommend the most effective NDE method to use on new impellers in order to preclude acceptance of impellers containing such defects.

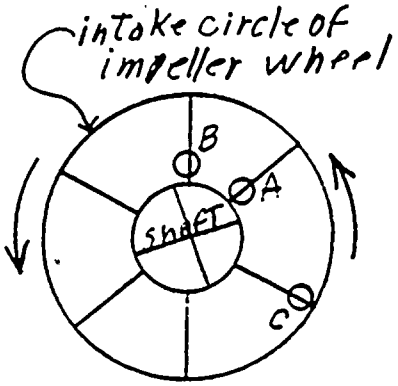

Figure 1.

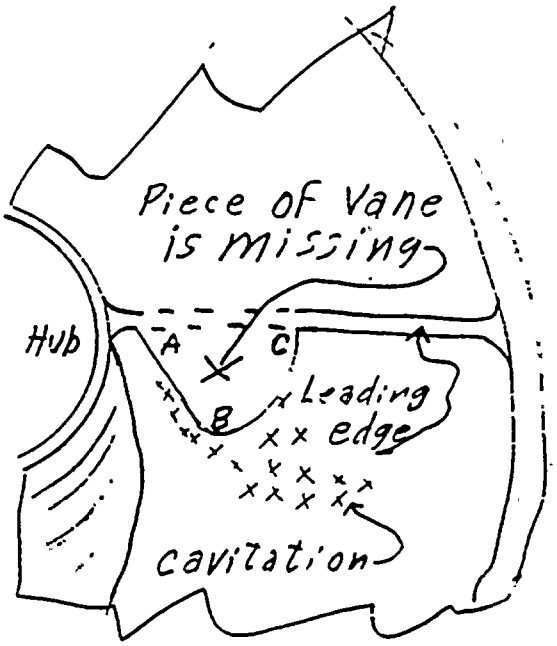

Figure 2.

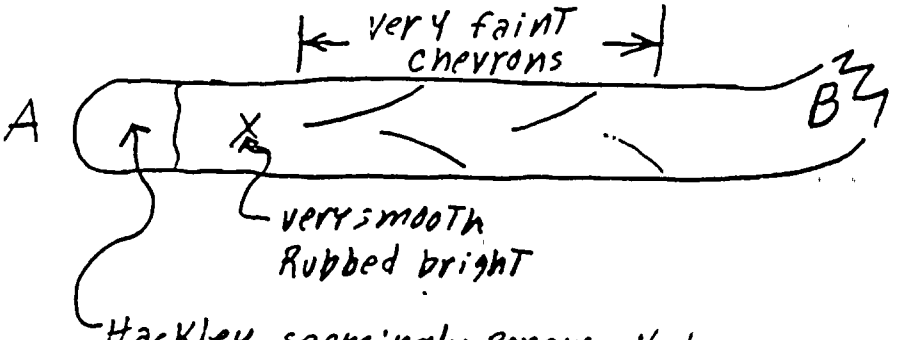

Figure 3A

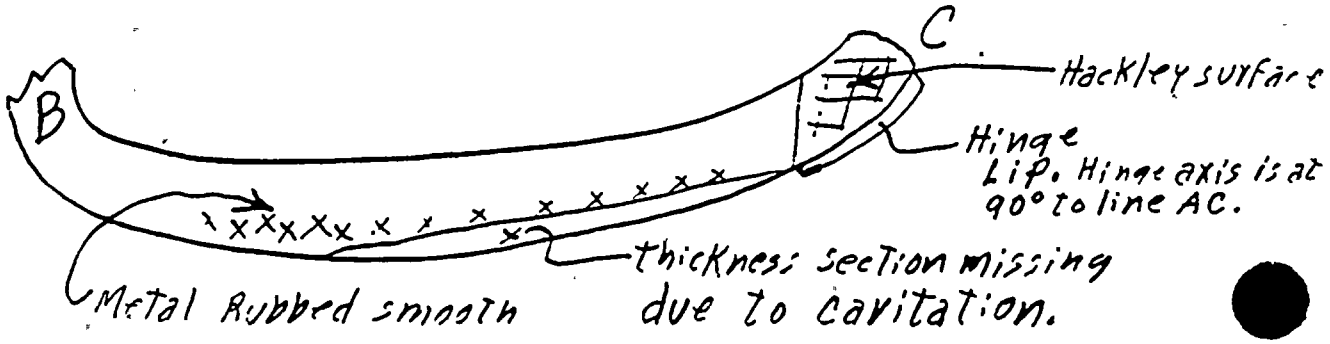

Figure 3B

APPENDIX G

SAFETY EVALUATION COVER SHEET

PLANT: Nine Mile Point Unit 1

SYSTEM: Feedwater

MODIFICATION TITLE: Analysis of Lost Part in Feedwater System

REVISED
AS APPROVED BY
SORC
on 2/25/88

MODIFICATION NUMBER: N/A

MAJOR ORDER NUMBER: N/A

SAFETY EVALUATION NUMBER: 88-009

REVISION NUMBER: 1

Revision 1 incorporates SORC's comments from Revision 0.

PREPARED BY: Denise J. Wolniak — Licensing Engineer — Feb. 26, 1988 — Date

REVIEWED BY: N/A — Project Engineer — Date

RC 2/26/88 C. W. K. Smith — Lead Engineer — 2/26/88 — Date

M. A. Mroz — Lead Engineer - Safety Analysis — 2/26/88 — Date

APPROVED BY: M. P. M. A. F. Fallon Jr. — Manager, Licensing — 2/26/88 — Date

SORC REVIEW: Date: 2/25/88

Accepted as Submitted _____ Accepted as Revised ✓ Rev 0

Disapproved _____

SRAB REVIEW Date: _____

Concurs _____ Does Not Concur _____

RECEIVED

FEB 26 1988 -3

S.R.A.B

4283G

NT-100.B-2
Rev. 5 11/87

1. MODIFICATION TITLE: Analysis of Lost Part in Feedwater System

2. MODIFICATION BACKGROUND AND SCOPE:

On December 19, 1987, NMP1 experienced a feedwater transient. Upon investigation it was discovered that the #13 feedwater pump impeller was damaged. This damage resulted in the dislocation of a triangular piece or pieces of the impeller the approximate total size of 1-3/4" x 1-7/32" x 1-7/8". This evaluation assumes that the part/parts are in the feedwater piping and can travel with system flow. The purpose of this evaluation is to determine the possible safety consequences this lost part may create and if an unreviewed safety question exists.

3. ANALYSIS:

After dislodging from the impeller, the lost part could eventually travel with the feedwater flow back to the reactor vessel. In order to determine possible safety consequences, critical components in the system flow path will be analyzed.

The first components that could be affected by the lost part are the #13 feedwater flow control valves. Calculations have shown that the part would be capable of ascending the vertical run prior to these valves. Once at the valves, the part could become lodged such that a flow control valve could fail in its "as is" position. Should this occur at full power, the feedwater flow control system could, under normal conditions, regulate reactor water level utilizing the remaining flow control valves. When postulating worse case conditions, inadequate or excessive feedwater flow from the #13 feedwater shaft driven pump could be possible. The FSAR transient analyses, Feedwater Controller Failure - Maximum Demand and Feedwater Controller Malfunction (Zero Demand) bounds this worst case scenario and, therefore, demonstrates that an unreviewed safety question does not exist. Additionally, the FSAR analysis assumes all 4 flow control valves experience a simultaneous failure instead of one as currently discussed. The probability of occurrence and consequences for this type of accident, therefore, remains unaffected.

After passing through the flow control valves, the lost part could become lodged at the inlet to one of the 5th stage feedwater heaters. Reduced heat transfer capacity due to the largest possible sized part would be minimal and bounded by the FSAR analyses "Loss of Feedwater Heating." The U tubes of the heaters are .603" in diameter. Therefore, in order to proceed toward the vessel, the lost part would have to corrode to a maximum size of 2" x .603".

Should the lost part be (or corrode to) less than .603" width, the next downstream components that may be affected are the feedwater isolation valves. The isolation valves utilized in the feedwater system are a check valve and gate valve. Engineering has reviewed the internal configurations of these safety-related valves and has determined that due to their designs, a lost part or pieces cannot become lodged in a position which could eventually prevent valve closure (memo: Corieri to Mosier, 1/15/88). The only possible way a part could adversely affect a valve is to be passing across the valve seat at the moment of valve

closure. Since the gate valve is motor driven, it will fully close in spite of any obstruction due to the force of the actuator. The check valve, however, seats on system backpressure and must be further analyzed.

The probability that a lost piece is traveling across the check valve seat at the exact time it seats is extremely low. However, since it has been identified, it must be evaluated to determine any potential effects it may have on accidents or malfunctions of equipment already analyzed in the FSAR or if new accidents or malfunctions could be created.

Lodging of a lost part in the check valve does not, by itself, create any new accidents. Additionally, there is a redundant isolation valve that would provide complete isolation should the part cause check valve leakage.

Numerous accidents are analyzed in the FSAR and all will remain unaffected by the possibility of the check valve jamming. Again, a redundant gate valve exists that will prevent any increase in offsite releases greater than those previously evaluated. In FSAR accidents analyzed, worst case failures were assumed that remain valid even in consideration of the presence of the lost part. The consequences and probabilities of accidents previously analyzed will, therefore, remain unaffected.

In addition to questions concerning postulated accidents, 10 CFR 50.59 also requires a determination as to whether the probability of occurrence or consequences of any malfunction of equipment important to safety previously evaluated in the FSAR is increased or new malfunction created. The Nine Mile 1 FSAR does not, in any accident analysis, discuss or assume the failure of a feedwater check valve. Therefore, all analyses and assumptions in the FSAR remain valid in regards to malfunctions of equipment. The possible jamming of the check valve does increase the probability of failure of the check valve to close. This probability of the check valve jamming is, however, so small as to negligibly affect the probability of a failure to isolate on demand. A quantitative assessment of this probability (as recommended by ANSI/ANS 52.1) is, however, difficult to perform and must therefore be based on good engineering judgment. Since a quantitative measure is absent, engineering has gone further with the evaluation by assuming the worst case accident conditions with an unseated check valve (Calc. #S12-31-PP1). The worst case conditions measured in the probability analysis are: 1) feedwater line break, 2) failure to isolate the gate valve, and 3) the piece is at the seat of the check valve when closing. Even by assigning an extremely conservative probability to the check valve jamming, the analysis estimated that the frequency of this worst case scenario was no greater than 8.8×10^{-12}/reactor year. By performing this calculation, the credibility of the check valve jamming is realized by comparing the frequency of this scenario to the design requirements of ANSI/ANS 52.1-1983. This ANSI Standard recommends that scenarios less than 10^{-6}/reactor year be considered incredible for design considerations. The calculated value of 8.8×10^{-12}/reactor year far exceeds this guide value in the conservative direction. Presence of the lost part does not, therefore, increase the consequences or probability of malfunction equipment important to safety.

The last obstruction before entering the reactor vessel is the feedwater spargers. The diameter of the orfices in each of the spargers is 1". The part, depending upon it orientation, may or may not become lodged a the sparger. Due to the size of the part, any feedwater flow blockage that may occur will be negligible compared to the HPCI design flow rate of 3600 gpm.

After much time, the lost part from the impeller may enter the reactor vessel. To analyze the consequences of this action, General Electric (GE) has performed a lost parts evaluation (G-EAI-8-003, dated 1/12/88). The results of this evaluation concludes that two previously performed lost parts analyses reports are applicable to the missing impeller piece and the conclusions of these reports are not impacted by the additional piece. General Electric did not recommend control rod friction testing be performed for this lost part.

The conclusions of the referenced reports state that the lost part will not present a safety concern in terms of:

1. The potential for fuel bundle blockage and subsequent fuel damage.

2. The potential for control rod interference.

3. The potential for corrosion or other chemical reaction with reactor materials.

4. The potential for main steam isolation valve (MSIV) interference.

Based upon GE's analysis, entrance of the lost part into the vessel is not a safety concern.

4. CONCLUSION:

Based upon the above analyses, the existence of the lost part from the feedwater pump impeller does not present a safety concern. Required HPCI components and containment isolation valves will not be adversely affected. The lost part has been additionally analyzed by GE in terms of its effect once inside the vessel. GE's analysis concluded that no safety concerns exists. Therefore, continued operation of the feedwater system with the lost part is not an unreviewed safety question.

CERTIFICATION OF
COMPLIANCE TO NRC STANDARDS (10CFR50.59)

Modification Title: Analysis of Lost Part in Feedwater System Mod. Number: N/A

Safety Evaluation Number: 88-009 Revision: 1

A. Is the probability of occurrence or the consequences of an accident or malfunction of equipment important to safety previously evaluated in the safety analysis report increased? No, the loss of feedwater heating and feedwater controller malfunction analyses are unaffected by the presence of the lost part. The possibility of the check valve leaking is so small as to negligibly effect the probability of a failure to completely isolate on demand.

B. Does the modification create the possibility for an accident or malfunction of a different type than any evaluated in the safety analysis report? No new scenarios are created by the lost part as demonstrated by the GE analysis. Additionally, any feedwater components that may be degraded are bounded by existing analyses.

C. Is the margin of safety reduced, as defined in the basis for any Technical Specification? No, the #13 flow control valves are not part of HPCI and any postulated flow blockage of a heater and sparger will not reduce HPCI flow below requirements. Additionally, GE has determined fuel bundle flow blockage will be less than 10%. This is far less than the 80% blockage required for fuel damage.

Based on A, B and C above, this modification does not constitute an unreviewed safety question.

D. Are changes required in the Technical Specifications incorporated in the license (Yes/No)? If yes, describe No.

CERTIFICATION OF
COMPLIANCE TO NRC STANDARDS
(10CFR50.59) (NT-100.B) (Cont.)

E. Will the proposed change, test or experiment result in a significant increase in any adverse environmental impact previously evaluated in the FES-OL, environmental impact appraisals, or in any decisions of the Atomic Safety and Licensing Board? No.

F. Will the proposed change, test or experiment result in a significant change in effluents or power level? No.

G. Will the proposed change, test or experiment concern a matter not previously reviewed and evaluated in the documents specified in question "E" above, which may have a significant adverse environmental impact? No.

H. Will the proposed change constitute a decrease in the effectiveness of the NMP2 Environmental Protection Plan? N/A

Based on E, F, G and H above, this modification does not constitute an unreviewed environmental question.

I. Are changes required in the Environmental Protection Plan (Appendix B to NMP#2 Operating License)? (Yes/No) If yes, describe N/A

SAFETY ANALYSIS REVIEW VERIFICATION

SAFETY EVALUATION NUMBER 88-009 REVISION 1

TITLE: Analysis of Lost Part in Feedwater System

	APPROVALS	DATE
1. ALARA review completed per NT-100.A	N/A*	
2. EQ review, completed per NEL-028 or PG201		
3. Fire Protection analysis completed per NT-100.D		
4. 10CFR Appendix R compliance review completed per NT-100.D		
5. Fuel Analysis Review completed		
6. Changes to FSAR required ____ Yes ____ No		
7. Changes to Control Room Habitability study conclusions required (If yes, explain) ____ Yes ____ No		
8. Equipment Clearance Review Completed	N/R	
9. Category II over I Review Completed	N/R	
10. Jet Impingement Review Completed	N/R	

Concurrence: Denise J. Wolniak 2/26/88
Licensing Engineer Date

*Signatures from Rev. 0 remain applicable.

NT-100.B-2
Rev. 5 11/87

SAFETY ANALYSIS REVIEW VERIFICATION

SAFETY EVALUATION NUMBER 88-009 REVISION 0

TITLE: Analysis of Lost Part in Feedwater System

		APPROVALS	DATE
1.	ALARA review completed per NT-100.A	N/A	
2.	EQ review completed per NEL-028 or PG201		
3.	Fire Protection analysis completed per NT-100.D		
4.	10CFR Appendix R compliance review completed per NT-100.D		
5.	Fuel Analysis Review completed	JE Mitchell	2/22/88
6.	Changes to FSAR required ____ Yes ____ No	N/A	
7.	Changes to Control Room Habitability study conclusions required (If yes, explain) ____ Yes ____ No		
8.	Equipment Clearance Review Completed		
9.	Category II over I Review Completed		
10.	Jet Impingement Review Completed		

Concurrence: Denise J. Wolmak 2/22
Licensing Engineer Date

FUEL ANALYSIS REVIEW CHECKLIST

UNIT 1

MODIFICATION TITLE: ANALYSIS OF LOST PART IN FEEDWATER SYSTEM

MODIFICATION NUMBER: _____

SAFETY EVALUATION NO. 88-009 Rev.0

The following questions must be considered in performing the fuel analysis review of the proposed modification.

1. Water Chemistry

   A. Does the modification affect, or have the potential to affect, fuel water chemistry requirements as specified in the applicable fuel fabrication contract?

      Yes ____ No ✓ N/A ____

   B. Does the modification increase the potential for introduction of foreign material into the fuel assemblies?

      Yes ✓ No ____ N/A ____

   C. If the water chemistry requirements are affected, or the likelihood of foreign material introduction into the fuel assemblies is increased, have the necessary actions been taken to assure fuel integrity is not unduly compromised?

      Yes ✓ → SEARCH MADE, ANALYSIS OBTAINED FROM GE, NOT A UNIQUE HARDWARE. No ____ N/A ____

2. Licensing Analysis

   A. Does the modification affect any input to the applicable reload licensing analysis?

      Yes ____ No ✓ N/A ____

   B. Does the modification affect the input data to the applicable 10CFR50 Appendix K licensing analysis?

      Yes ____ No ✓ N/A ____

   C. Does the modification affect the validity of other FSAR fuel related safety analyses?

      Yes ____ No ✓ N/A ____

FUEL ANALYSIS REVIEW CHECKLIST (Continued)

D. If yes to any of the above, does the safety evaluation analysis section adequately address any changes in the licensing analysis results?

Yes ____ No ____ N/A ✓

3. Fuel Handling and Storage Specification

A. Does the modification affect the requirements of the applicable fuel handling and storage specification?

Yes ____ No ✓ N/A ____

B. If yes, have appropriate actions been taken?

Yes ____ No ____ N/A ✓

4. Other Concerns

A. Describe: None

B. Have appropriate actions been taken?

Yes ____ No ____ N/A ✓

23 FEB 88

Responsible Fuel Engineer Steven Hollingsworth
Assoc. Nucl. Engr.

Reviewed by: D E Nelson

Lead Engineer - Fuels

Reference: GE Analysis
G-EAI-8-003

NIAGARA MOHAWK

MODIFICATION REVIEW (SITE OPERATIONS REVIEW COMM.)

MODIFICATION TITLE: Analysis of Lost Part in Feedwater System | UNIT: ☒ 1 ☐ 2 ☐ SITE

DOCUMENT

DOCUMENT TITLE: Analysis of Lost Part in Feedwater System | DOCUMENT NUMBER: 88-009 Rev 0

DOCUMENT TYPE ☐ CONCEPTUAL ENGINEERING PACKAGE ☒ FINAL SAFETY EVALUATION ☐ TECHNICAL SPECIFICATIONS

OTHER

ORIGINATOR: NAME	DEPARTMENT	DATE
Denise Wolniak	NT	2/24/88
PROJECT ENGINEER NAME	DEPARTMENT	DATE
N/A	ND	[redacted]

LOGGED BY SITE PLANNING: D. Lundeen/ltr DATE 2-26-88

SAFETY EVALUATION NUMBER (SE#): N 1 [redacted] 8 8 [redacted] 0 0 1 LE 0 0 5

REVIEW

NAME	ACCEPTED AS PRESENTED INITIALS	ACCEPTED AS PRESENTED DATE	ACCEPTED AS REVISED INITIALS	ACCEPTED AS REVISED DATE
1. SITE CONTACT				
2.				
3.				
4.				
6.				

SORC REVIEW

FINAL PRESENTED TO SORC BY D. Wolniak | DEPARTMENT Licensing | DATE 2/25/88

ACCEPTED BY SORC: ☐ AS SUBMITTED ☒ AS REVISED MEETING # 88-31

CHECK ONE, IF APPLICABLE:

☒ THIS MODIFICATION DOES NOT INVOLVE AN UNREVIEWED SAFETY QUESTION & DOES NOT INVOLVE A CHANGE TO TECHNICAL SPECIFICATIONS.

☐ THIS MODIFICATION INVOLVES AN UNREVIEWED SAFETY QUESTION OR A CHANGE TO TECHNICAL SPECIFICATIONS. PRIOR NRC APPROVAL SHALL BE OBTAINED.

CHECK ONE, IF APPLICABLE: N/A

☐ THE DOCUMENTS SUBMITTED FOR REVIEW NEED MORE DETAILED ENGINEERING OR REVISION. RETURN TO SORC FOR FURTHER REVIEW.

☐ THE MODIFICATION MAY PROCEED & BE INSTALLED AFTER SORC REVIEW OF THE FINAL SAFETY EVALUATION

SORC CHAIRMAN T J Perkins DATE 2/25/88 | FOR MAIL CONTROL USE ☐ SORC REVIEW N/A INT.

LOGGED COMPLETE BY SITE PLANNING: D. Lundeen/ltr DATE 2-26-88

SRAB REVIEW

☐ ACCEPTED BY SRAB: ☐ ACCEPTED AS SUBMITTED ☐ AS REVISED MEETING DATE

SRAB CHAIRMAN DATE | FOR MAIL CONTROL USE ☐ SRAB REVIEW N/A INT.

LOGGED CLOSED BY SITE PLANNING DATE

313-238 SYMBOL NO. 56-32 [illegible]

INTERNAL CORRESPONDENCE
FORM 112-2 R 02 80 55-01-013

NIAGARA MOHAWK

UNIT 2

FROM A. F. Zallnick, Jr.

DISTRICT Salina Meadows

DATE 2/26/88

T. Mr. T. J. Perkins
Chairman, Site
Operations Review
Committee

SUBJECT SAFETY EVALUATION
TITLE AND DOC. #

88-009, Rev.1

Analysis of Lost Part in Feedwater System

Attached for your information and use is the above subject Safety Evaluation which has been revised as approved by SORC on 2/25/88.

David MacKenzie FOR:AFZ
Manager, Nuclear Licensing

AFZ:jam

Attachment